Supporting Information for:
Step-Wise Changes in the Excited State Lifetime of $[Eu(D_2O)_9]^{3+}$ and $[Eu(DOTA)(D_2O)]^-$ as a Function of the Number of Inner-Sphere O-H Oscillators

Contents

$[Eu(H_2O)_9]^{3+}$ / $[Eu(D_2O)_9]^{3+}$

293 K

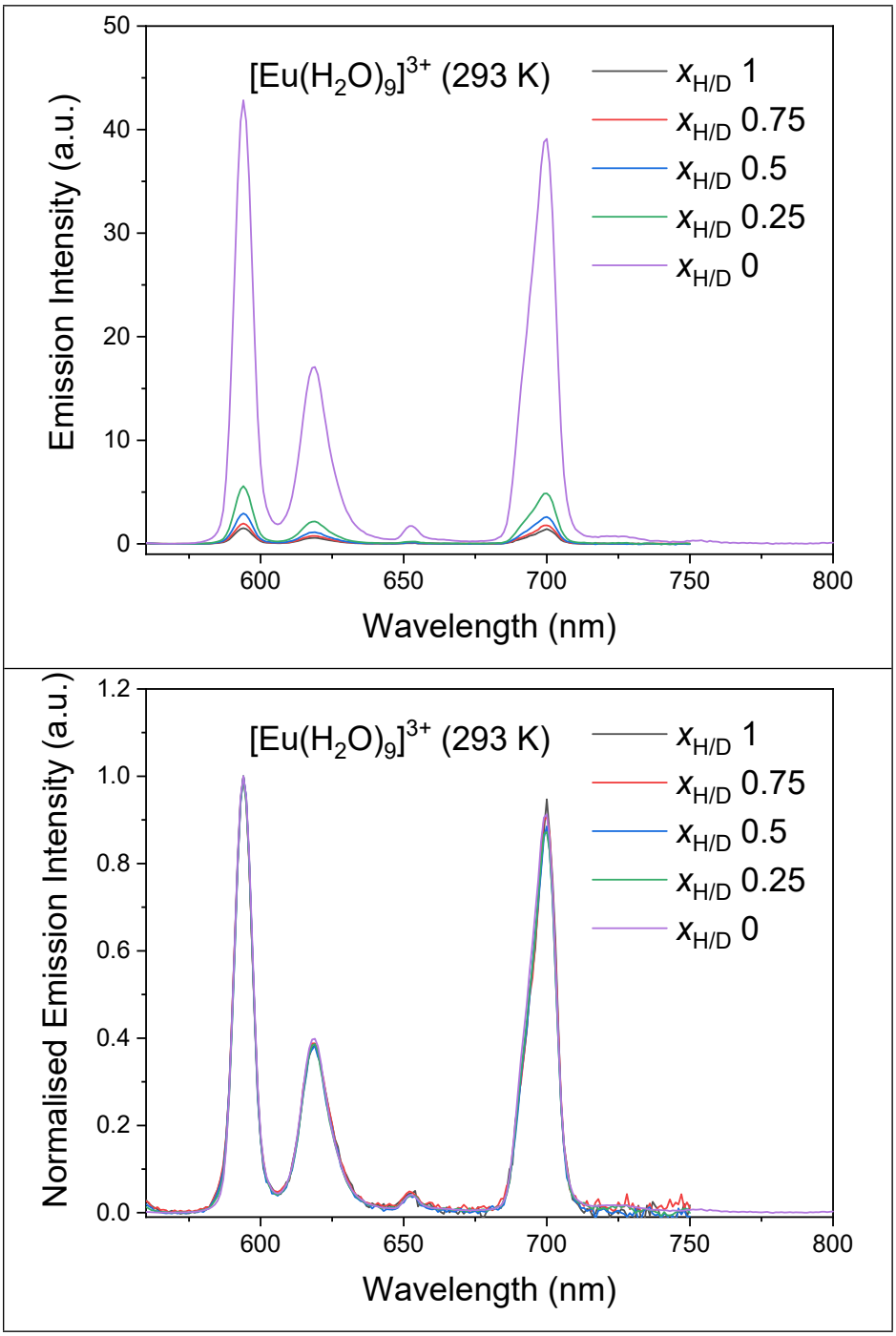

Figure S1. Emission spectra (top) and normalised emission spectra (bottom) of $[Eu(H_2O)_9]^{3+}$ in H_2O/D_2O mixtures in solution at 293 K. Emission slits were kept at 5 nm.

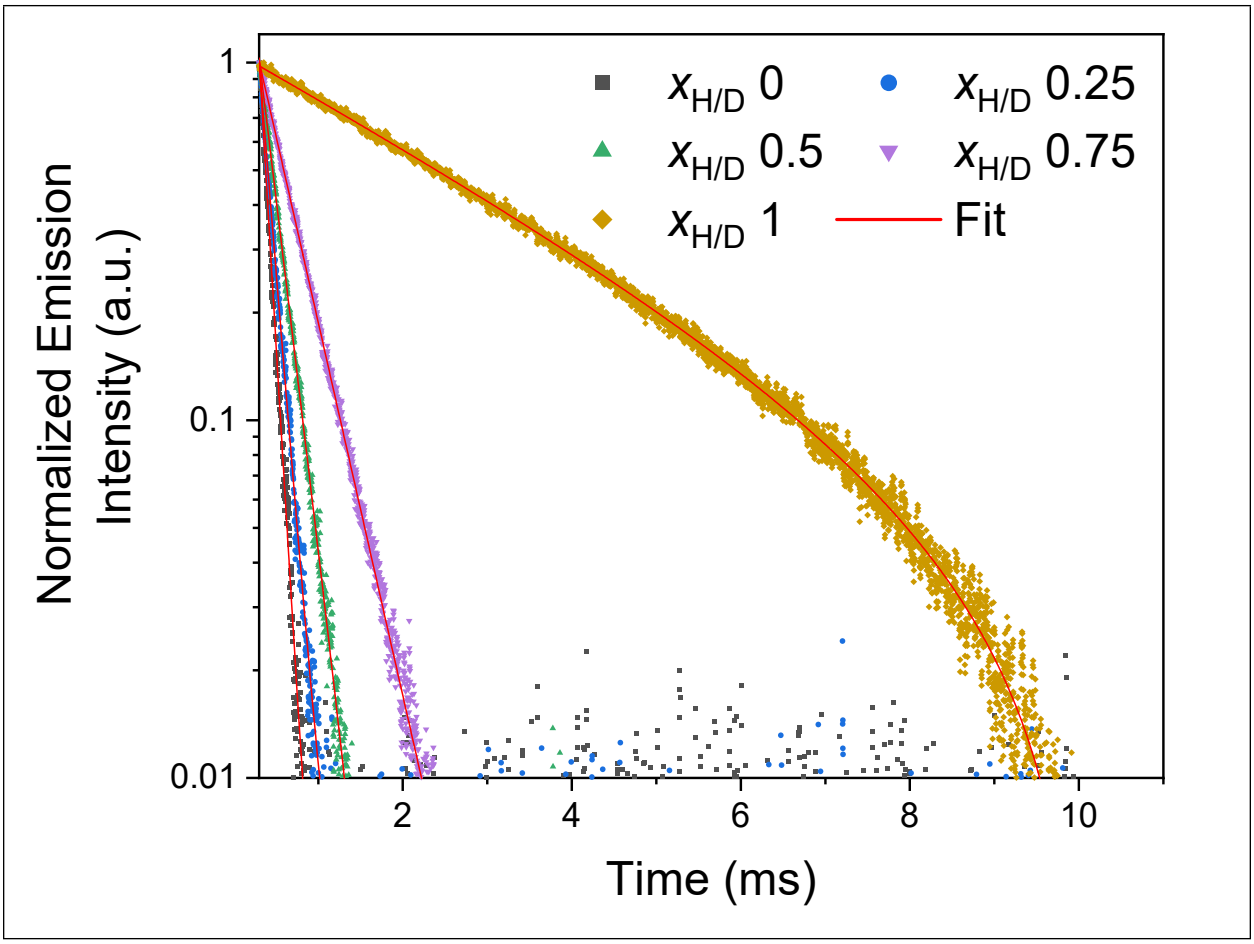

Figure S2. Emission decay traces of $[Eu(H_2O)_9]^{3+}$ in H_2O/D_2O mixtures in solution at 293 K. Data has been fitted to mono-exponential decay function.

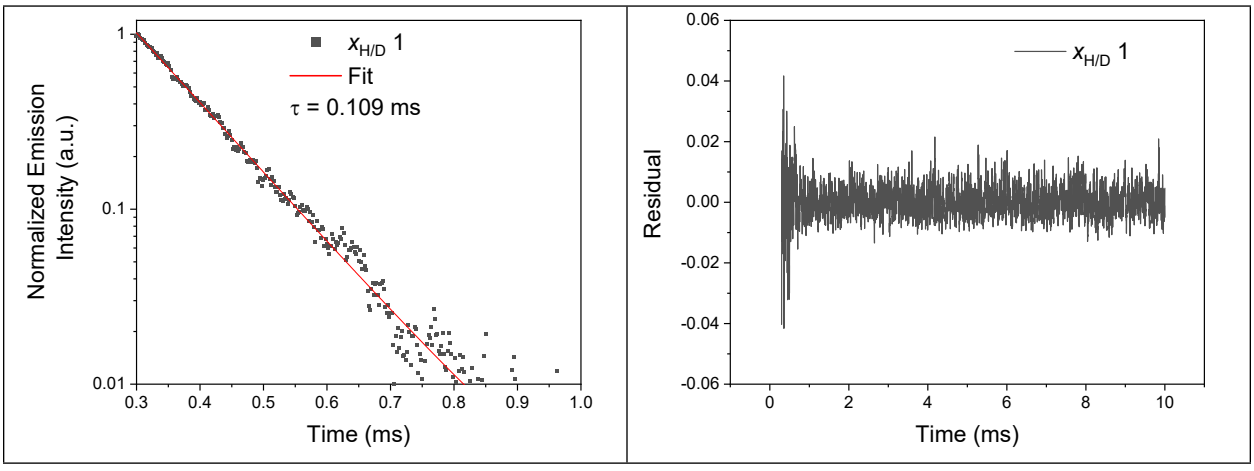

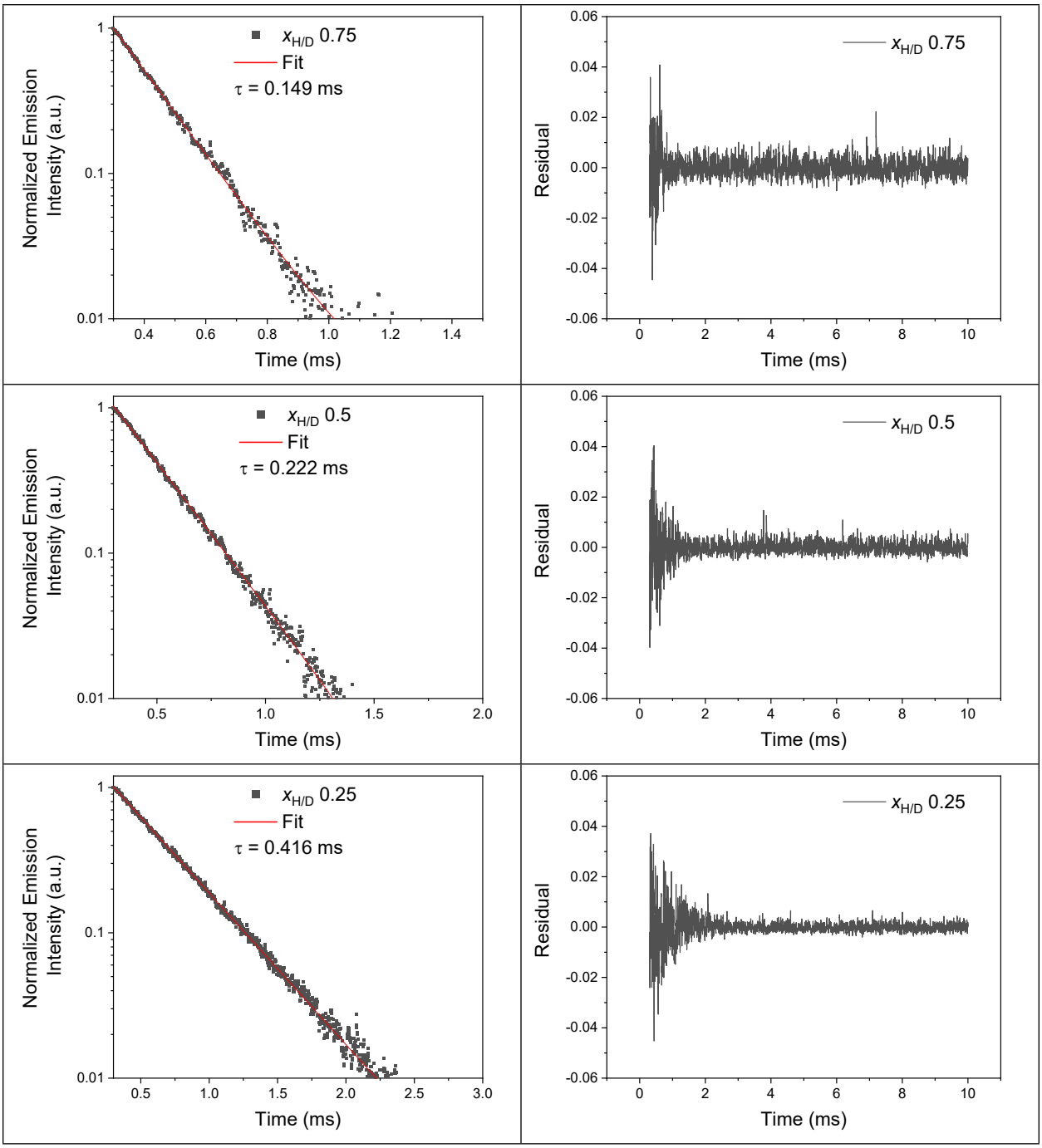
Normalized Emission Intensity (a.u.)
Time (ms)
$x_{H/D}$ 0.75
Fit
τ = 0.149 ms
Residual
$x_{H/D}$ 0.75
$x_{H/D}$ 0.5
Fit
τ = 0.222 ms
$x_{H/D}$ 0.5
$x_{H/D}$ 0.25
Fit
τ = 0.416 ms
$x_{H/D}$ 0.25

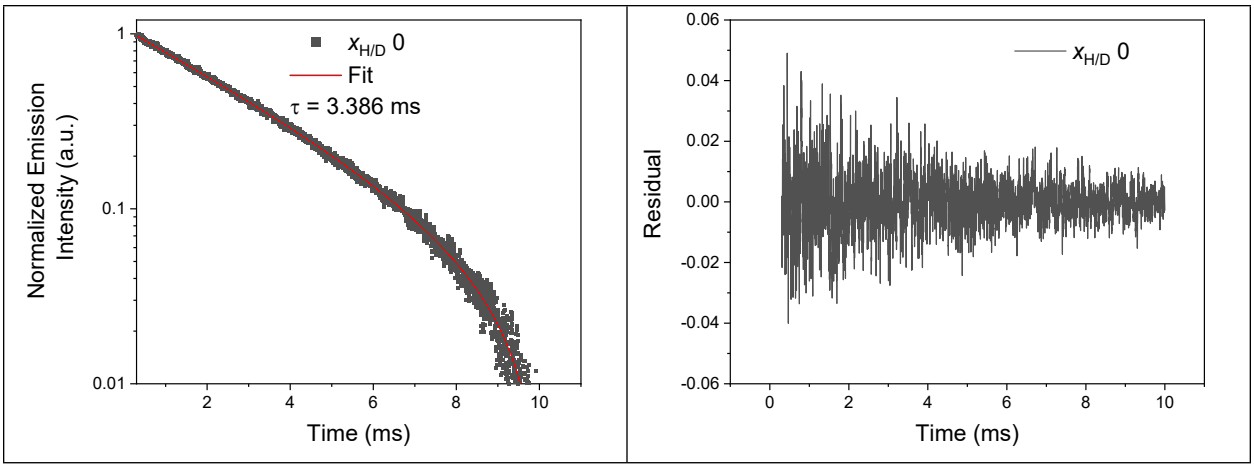

Figure S3. (left) Individual emission decay traces of $[Eu(H_2O)_9]^{3+}$ in H_2O/D_2O mixtures in solution at 293 K. Data has been fitted to mono-exponential decay function. (right) Residual between fit and data of fits.

Table S1. Fit parameters for $[Eu(H_2O)_9]^{3+}$ at 293 K.

$x_{H/D}$	A	τ
1	16.0 ± 0.10	0.109 ± 2.2E-4
0.75	7.45 ± 0.025	0.149 ± 2.0E-4
0.5	3.98 ± 0.0075	0.222 ± 2.2 E-4
0.25	2.07 ± 0.0021	0.416 ± 3.3E-4
0	1.13 ± 5.1E-4	3.386 ± 0.0048

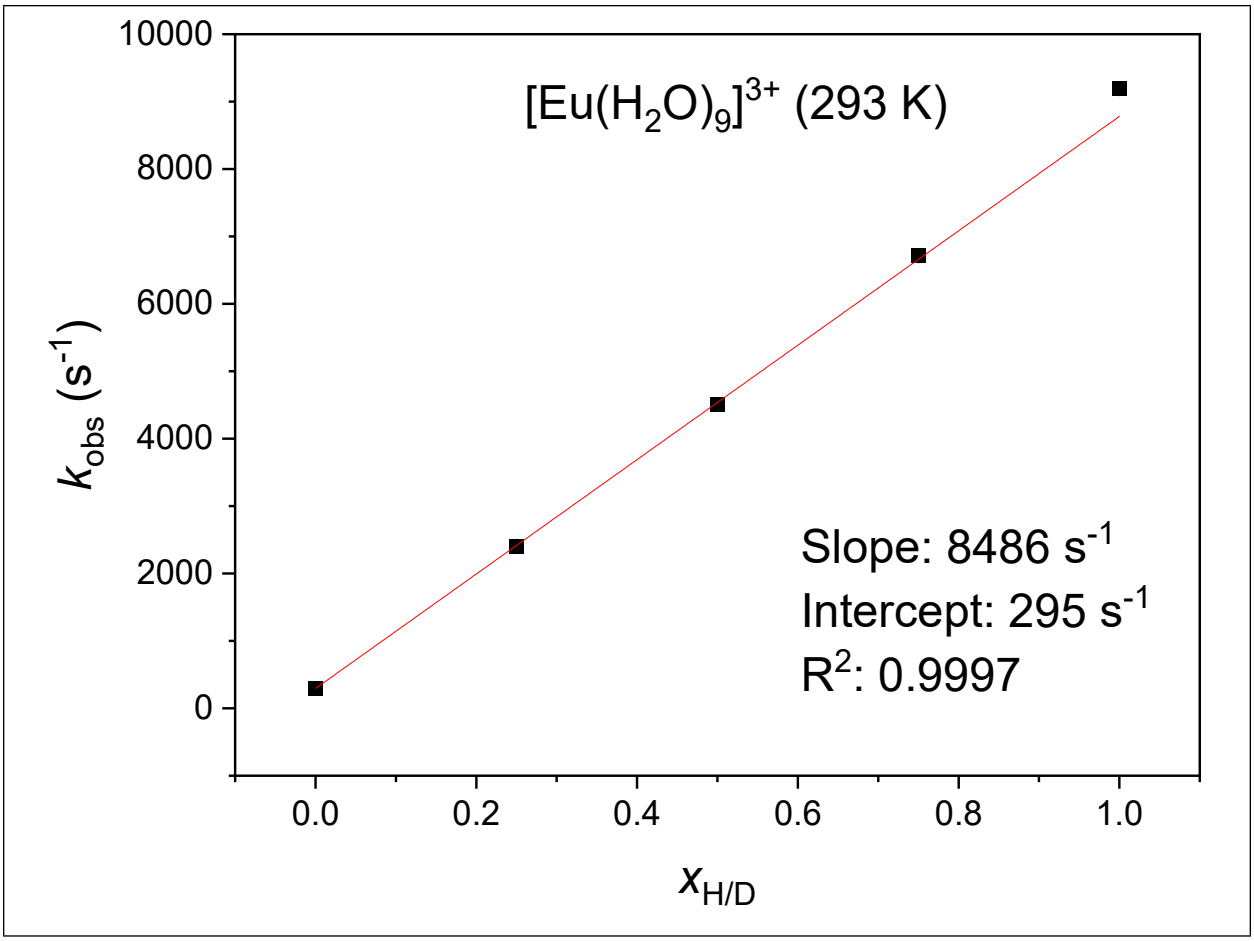

Figure S4. Observed rate of deactivation (k_{obs}) of the $^5D_0$ state of $[Eu(H_2O)_9]^{3+}$ in H_2O/D_2O mixtures in solution at 293 K. Data has been fitted with linear function

77 K

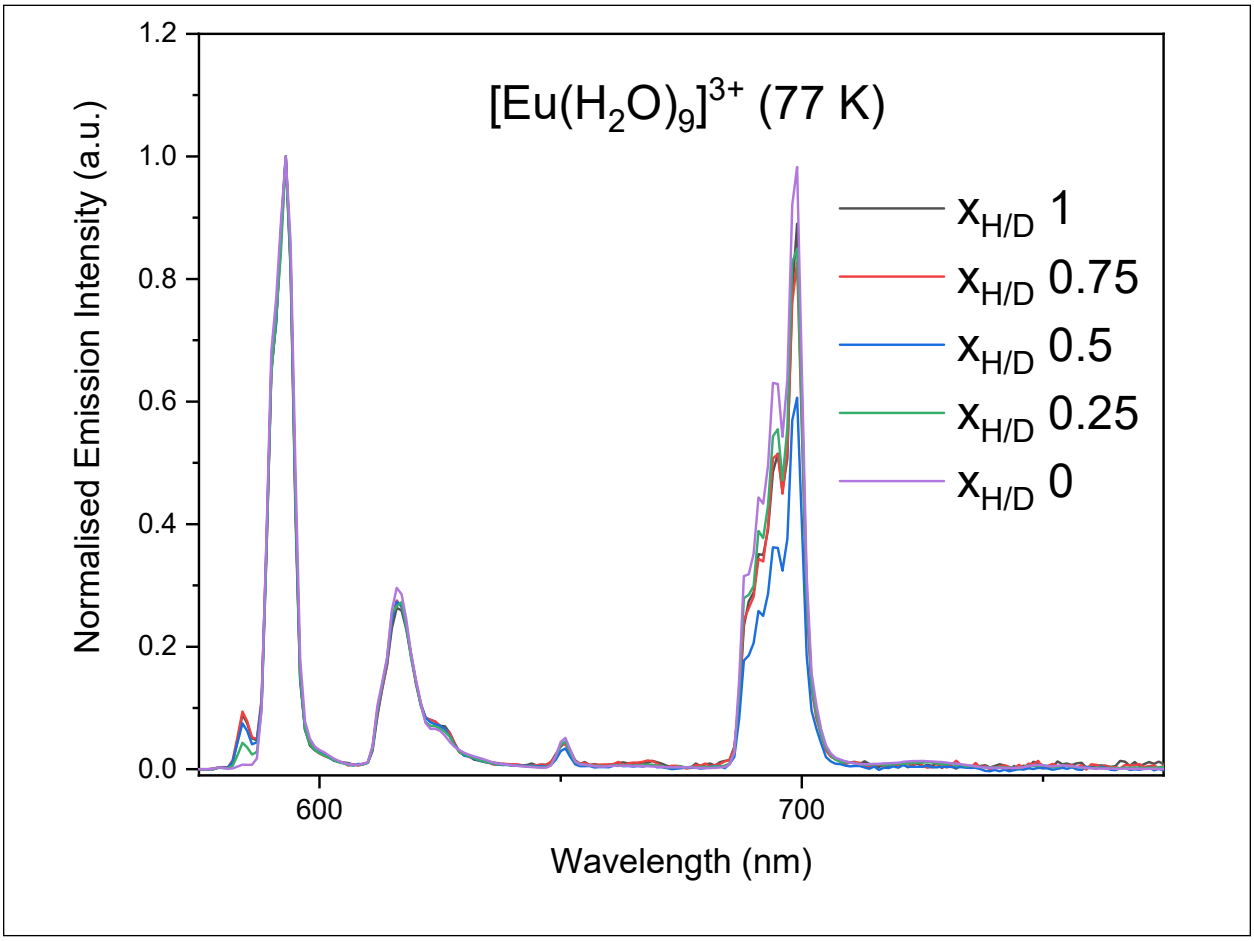

Figure S5. Normalised emission spectra (bottom) of $[Eu(H_2O)_9]^{3+}$ at in H_2O/D_2O mixtures in solution at 293 K. Emission slits were kept at 2 nm.

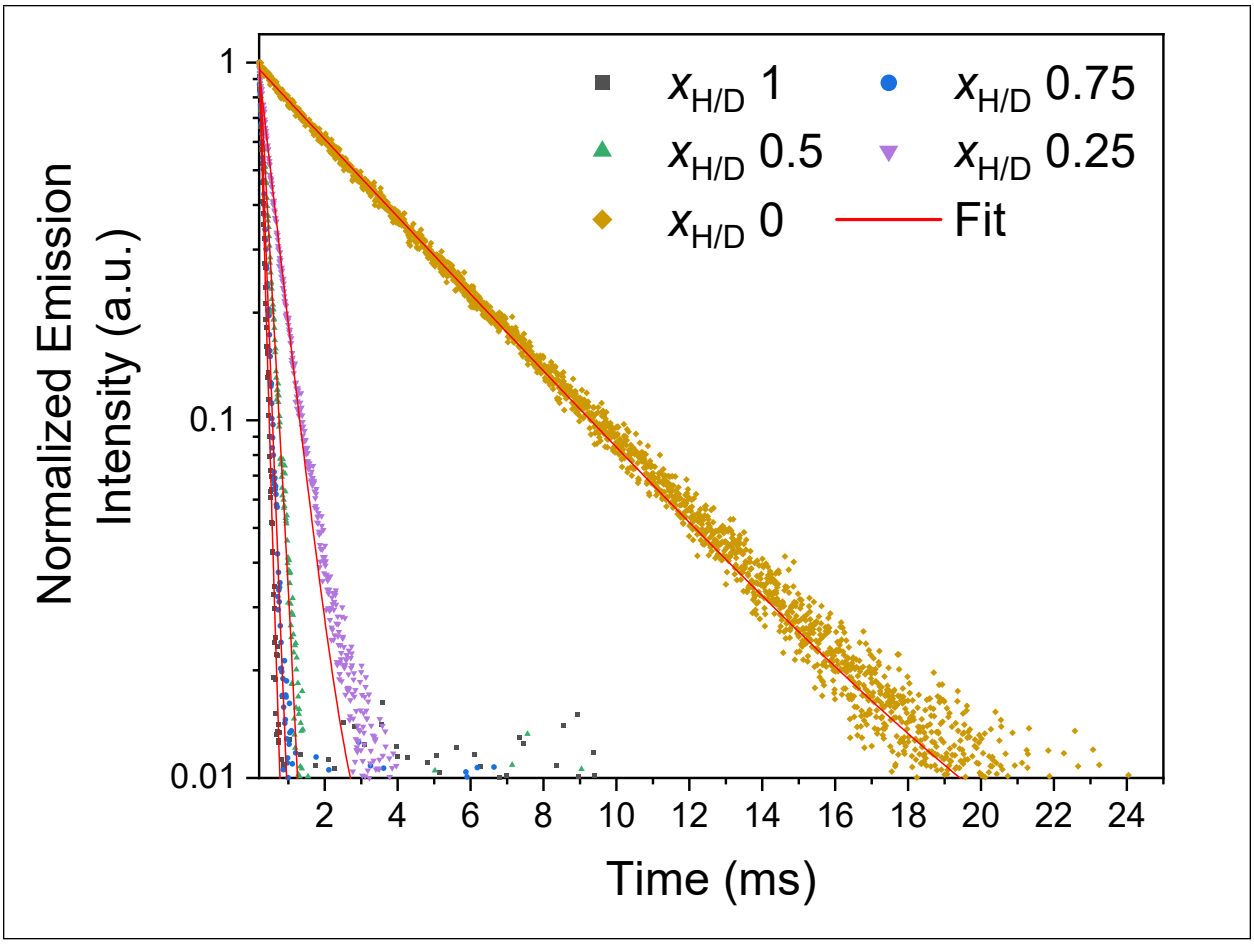

Figure S6. Emission decay traces of $[Eu(H_2O)_9]^{3+}$ in H_2O/D_2O mixtures in frozen solution at 77 K. Data has been fitted to mono-exponential decay function.

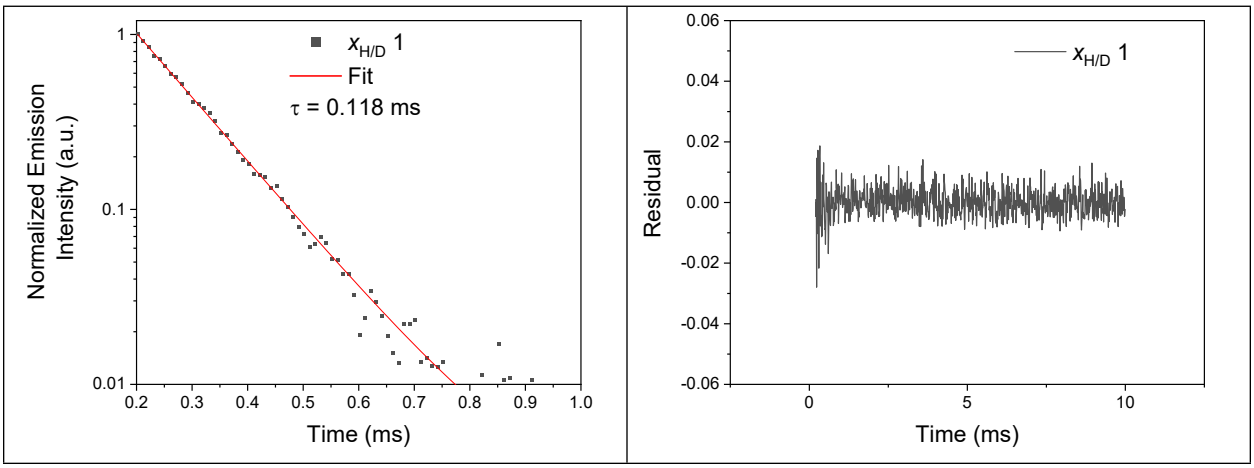

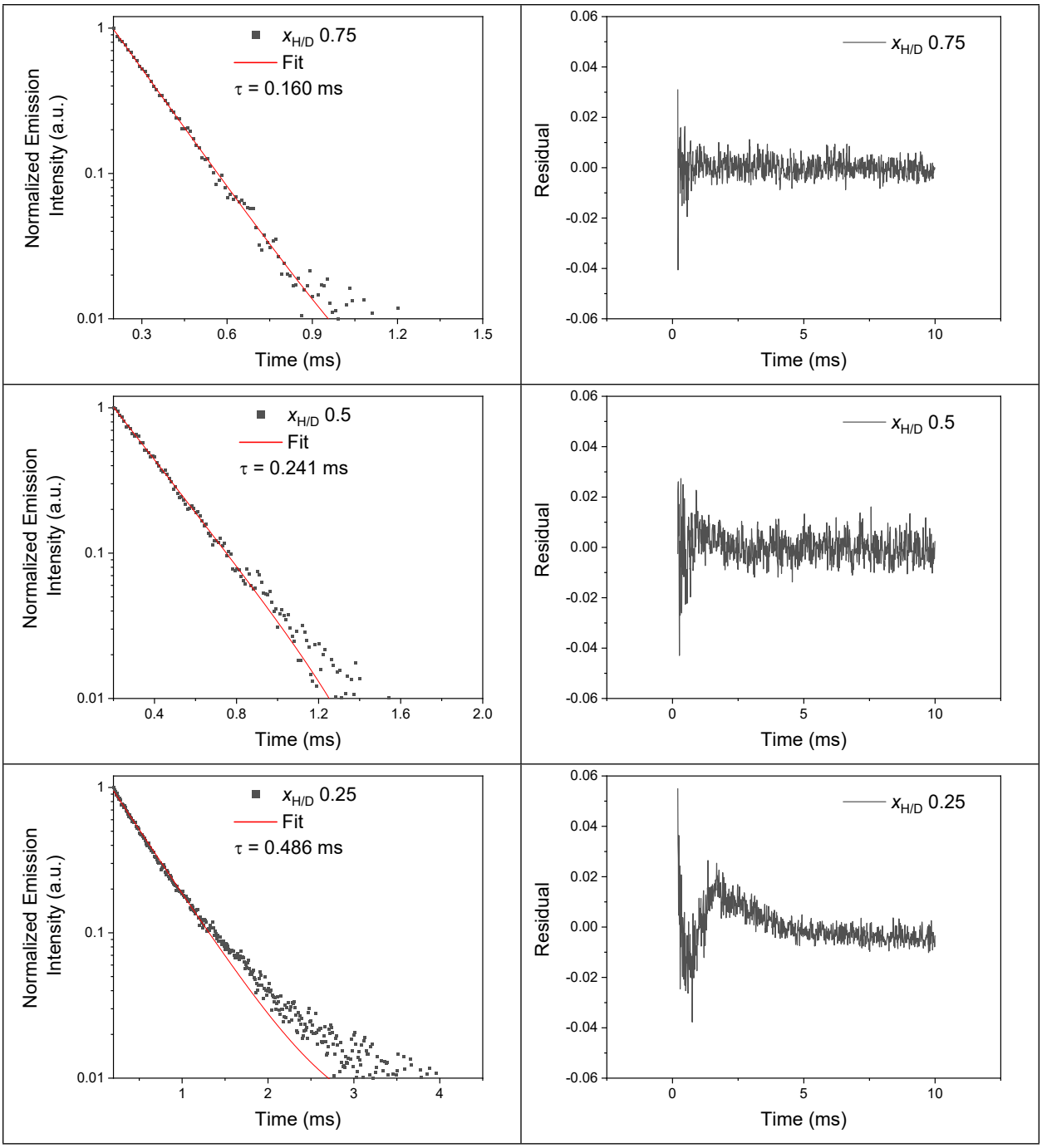
Normalized Emission Intensity (a.u.)
Time (ms)
$x_{H/D}$ 0.75
Fit
τ = 0.160 ms
Residual
$x_{H/D}$ 0.75
$x_{H/D}$ 0.5
Fit
τ = 0.241 ms
$x_{H/D}$ 0.5
$x_{H/D}$ 0.25
Fit
τ = 0.486 ms
$x_{H/D}$ 0.25

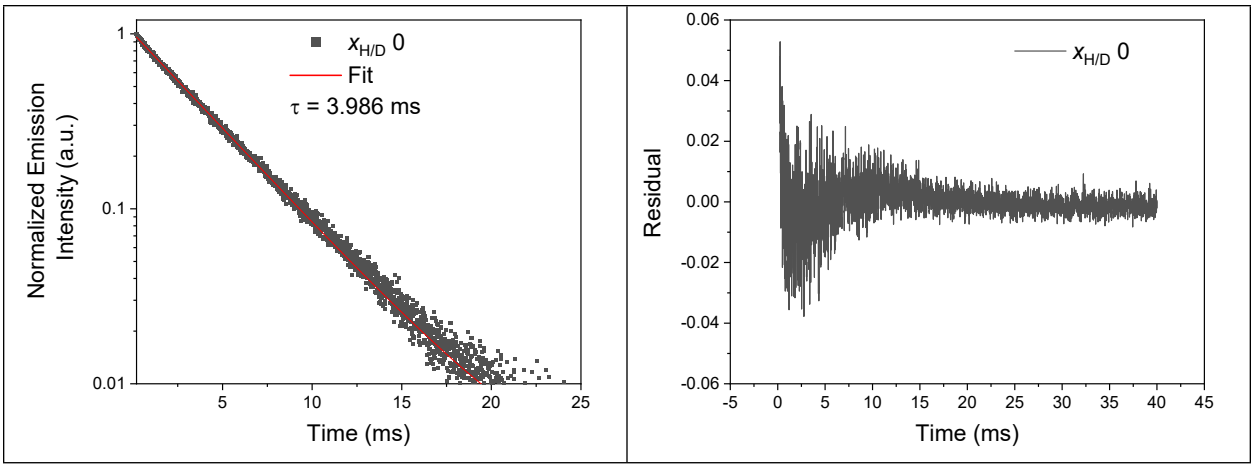

Figure S7. (left) Individual emission decay traces of $[Eu(H_2O)_9]^{3+}$ in H_2O/D_2O mixtures in frozen solution at 77 K. Data has been fitted to mono-exponential decay functions. (right) Residual between data and fit.

Table S2. Fit parameters for $[Eu(H_2O)_9]^{3+}$ at 77 K.

$x_{H/D}$	A	τ
1	5.50 ± 0.044	0.118 ± 4.3E-4
0.75	3.42 ± 0.018	0.160 ± 4.8E-4
0.5	2.33 ± 0.011	0.241 ± 8.4E-4
0.25	1.43 ± 0.0050	0.486 ± 0.0017
0	1.01 ± 7.1E-4	3.986 ± 0.0044

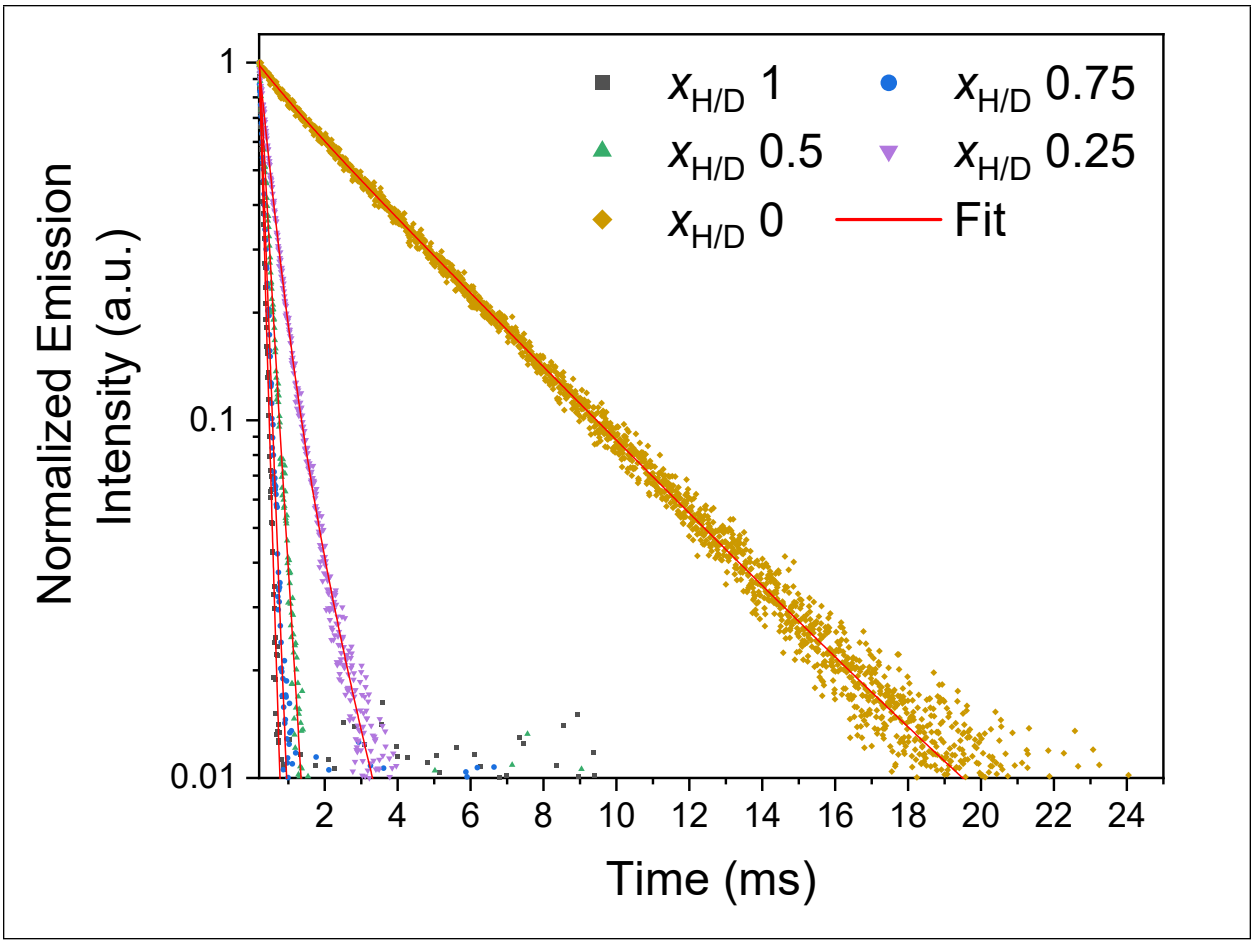

Figure S8. Emission decay traces of $[Eu(H_2O)_9]^{3+}$ in H_2O/D_2O mixtures in frozen solution at 77 K. Data has been fitted to mono-exponential (xH/D = 1, 0.75) or bi-exponential (xH/D = 0.5-0) decay functions.

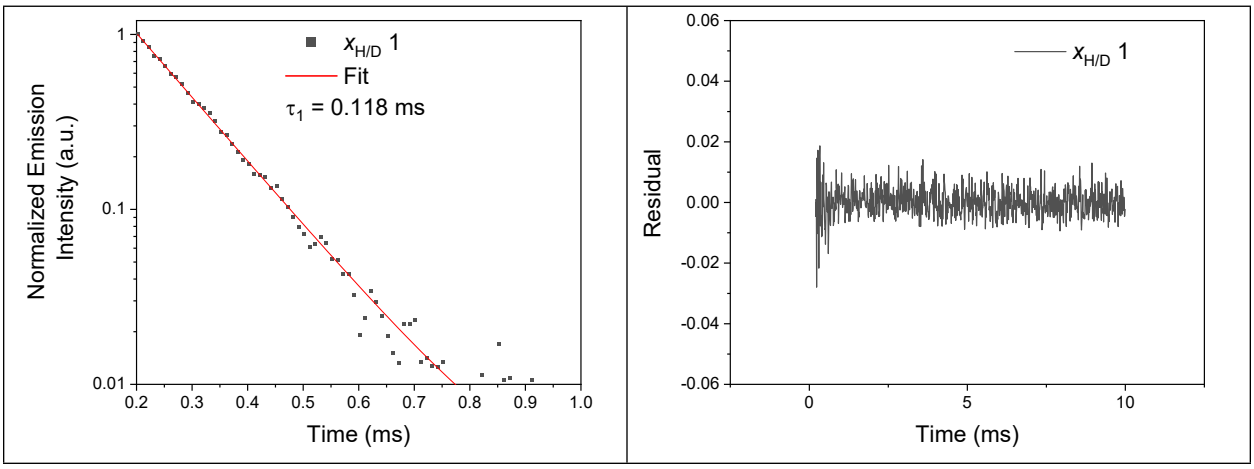

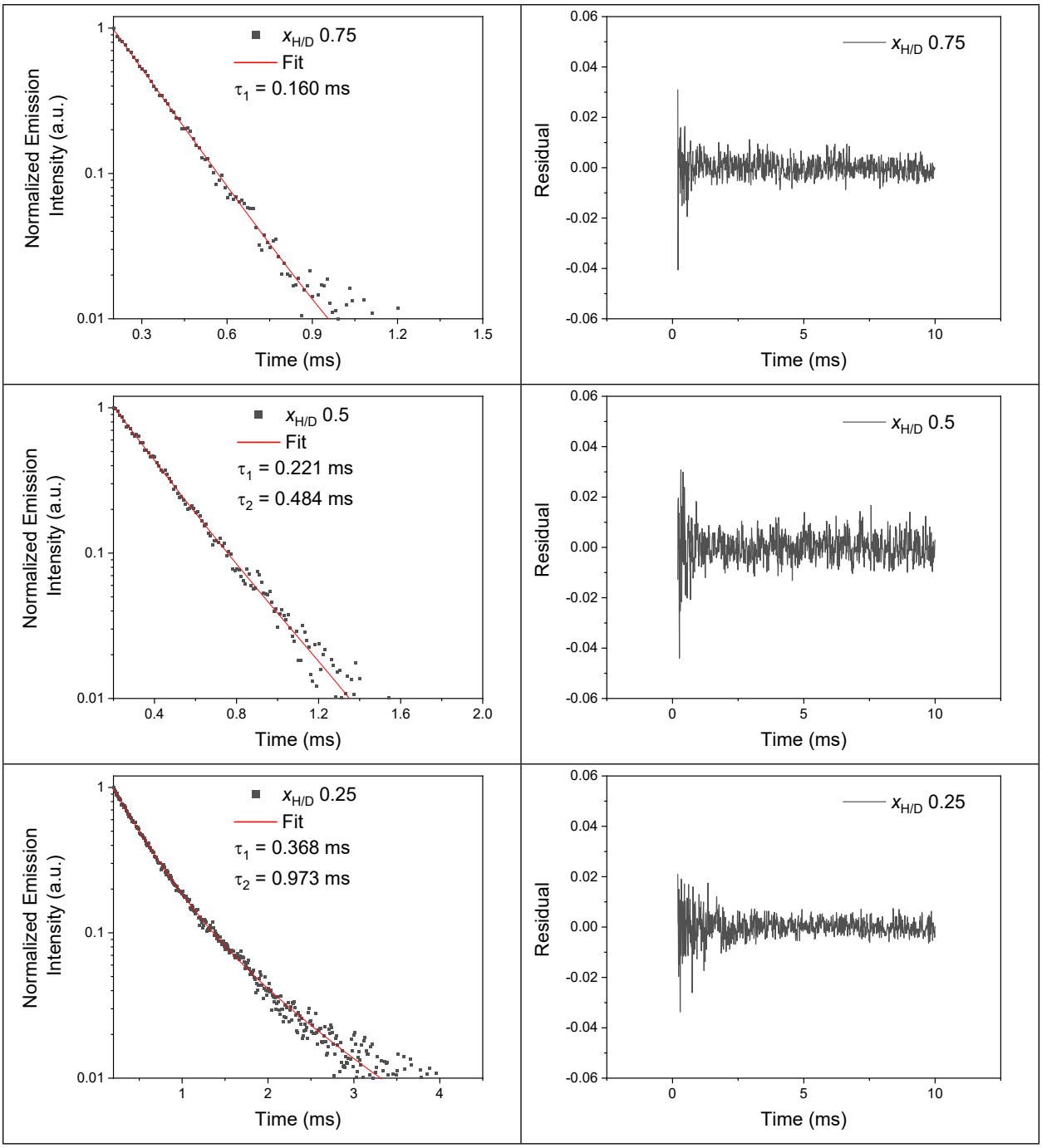
Normalized Emission Intensity (a.u.)
Time (ms)
$x_{H/D}$ 0.75
Fit
τ_1 = 0.160 ms
Residual
$x_{H/D}$ 0.75
$x_{H/D}$ 0.5
Fit
τ_1 = 0.221 ms
τ_2 = 0.484 ms
$x_{H/D}$ 0.5
$x_{H/D}$ 0.25
Fit
τ_1 = 0.368 ms
τ_2 = 0.973 ms
$x_{H/D}$ 0.25

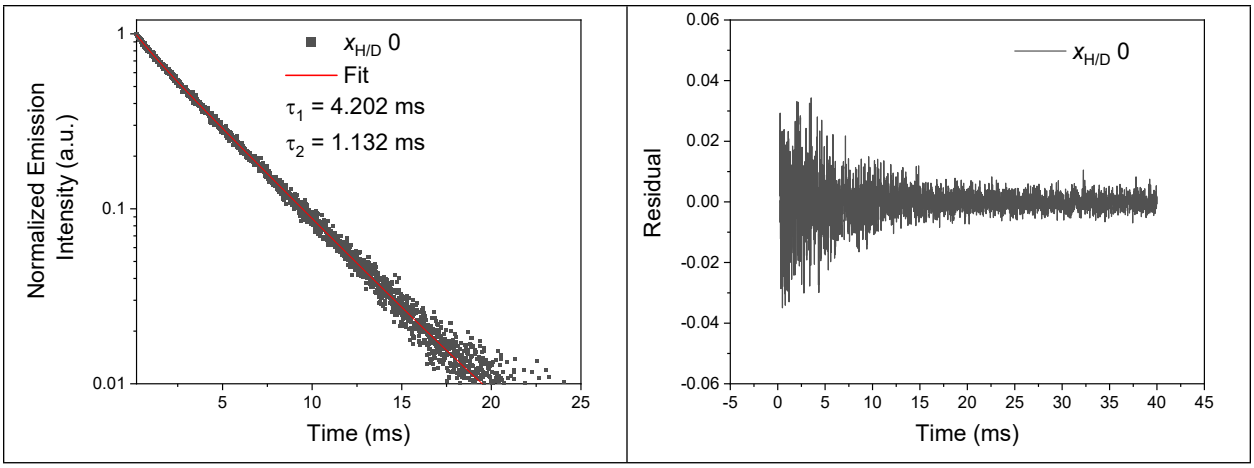

Figure S9. (left) Individual emission decay traces of $[Eu(H_2O)_9]^{3+}$ in H_2O/D_2O mixtures in frozen solution at 77 K. Data has been fitted to mono-exponential ($x_{H/D}$ = 1, 0.75) or bi-exponential ($x_{H/D}$ = 0.5-0) decay functions. (right) Residual of fit and data.

Table S3. Fit parameters for $[Eu(H_2O)_9]^{3+}$ at 77 K.

$x_{H/D}$	A_1	τ_1	A_2	τ_2
1	5.50 ± 0.044	0.118 ± 4.3E-4	-	-
0.75	3.42 ± 0.018	0.160 ± 4.8E-4	-	-
0.5	2.32 ± 0.06	0.221 ± 0.0060	0.136 ± 0.086	0.484 ± 0.097
0.25	1.31 ± 0.017	0.368 ± 0.0051	0.272 ± 0.0021	0.973 ± 0.032
0	0.104 ± 0.0042	1.132 ± 0.062	0.940 ± 0.0048	4.201 ± 0.013

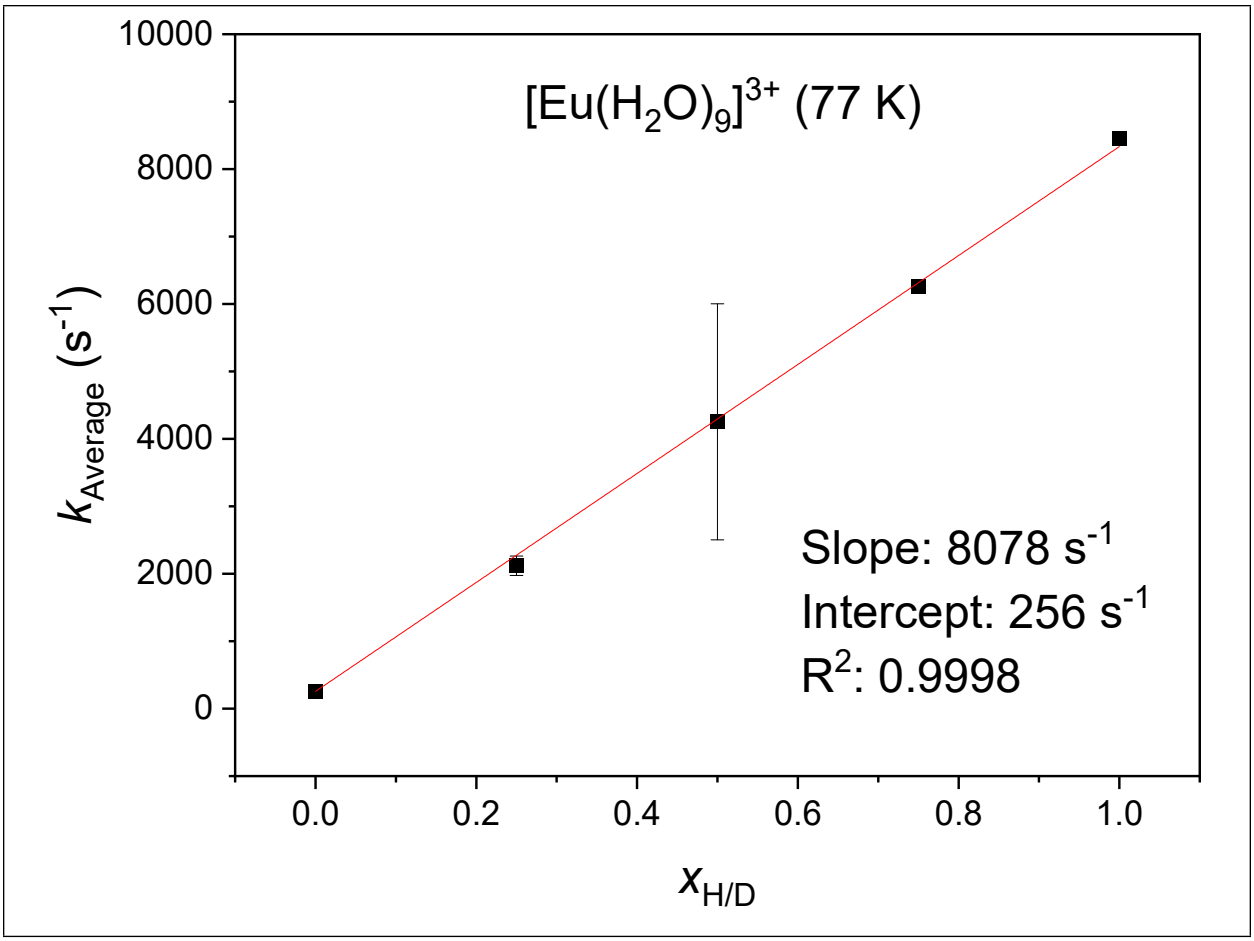

Figure S10. Average rate of deactivation ($k_{Average}$) of the $^5D_0$ state of $[Eu(H_2O)_9]^{3+}$ in H_2O/D_2O mixtures in frozen solution at 77 K obtained from multicomponent fits. Data has been fitted with linear function.

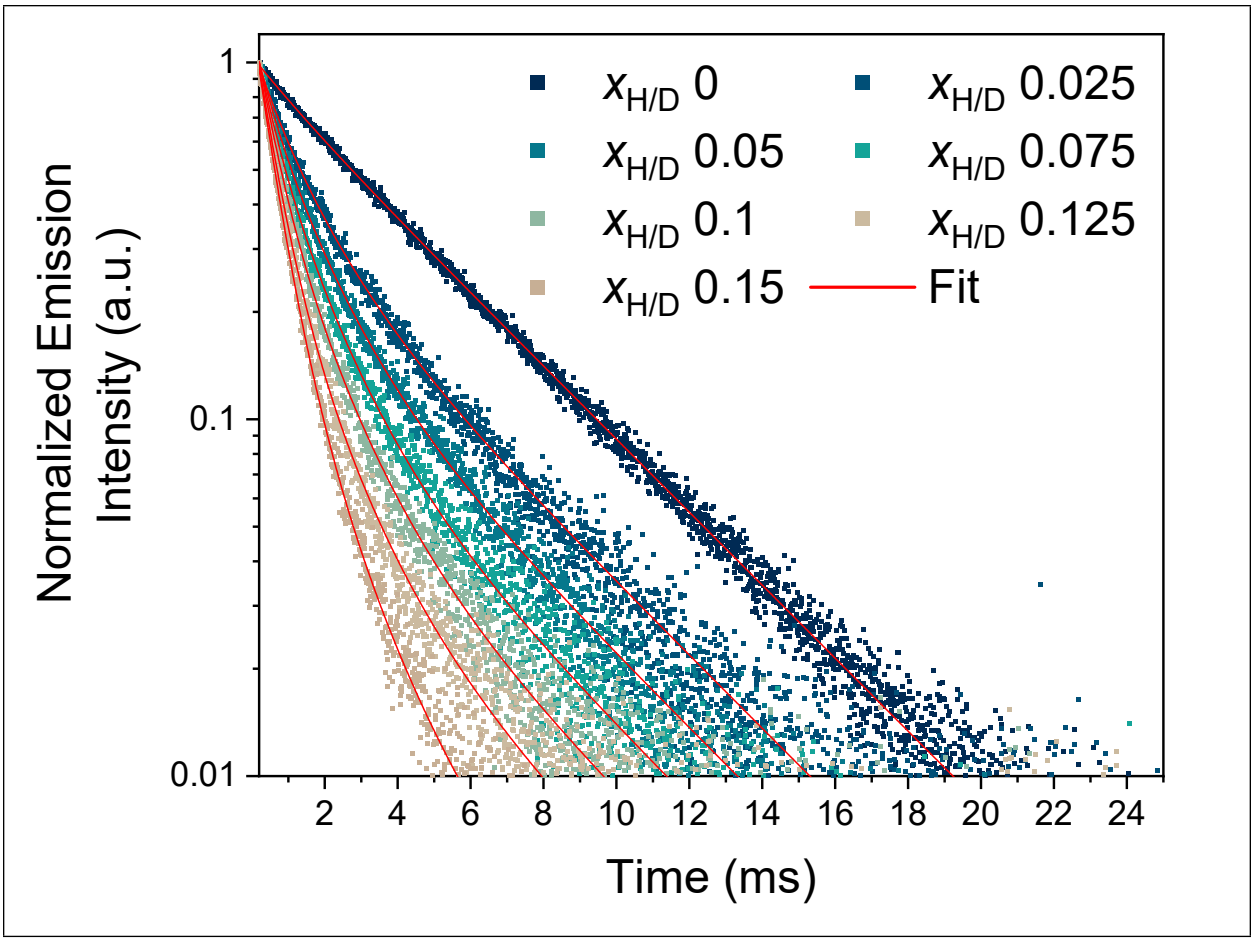

Figure S11. Emission decay traces of $[Eu(H_2O)_9]^{3+}$ in H_2O/D_2O mixtures in frozen solution at 77 K. Data has been fitted to tri-exponential decay using a global model.

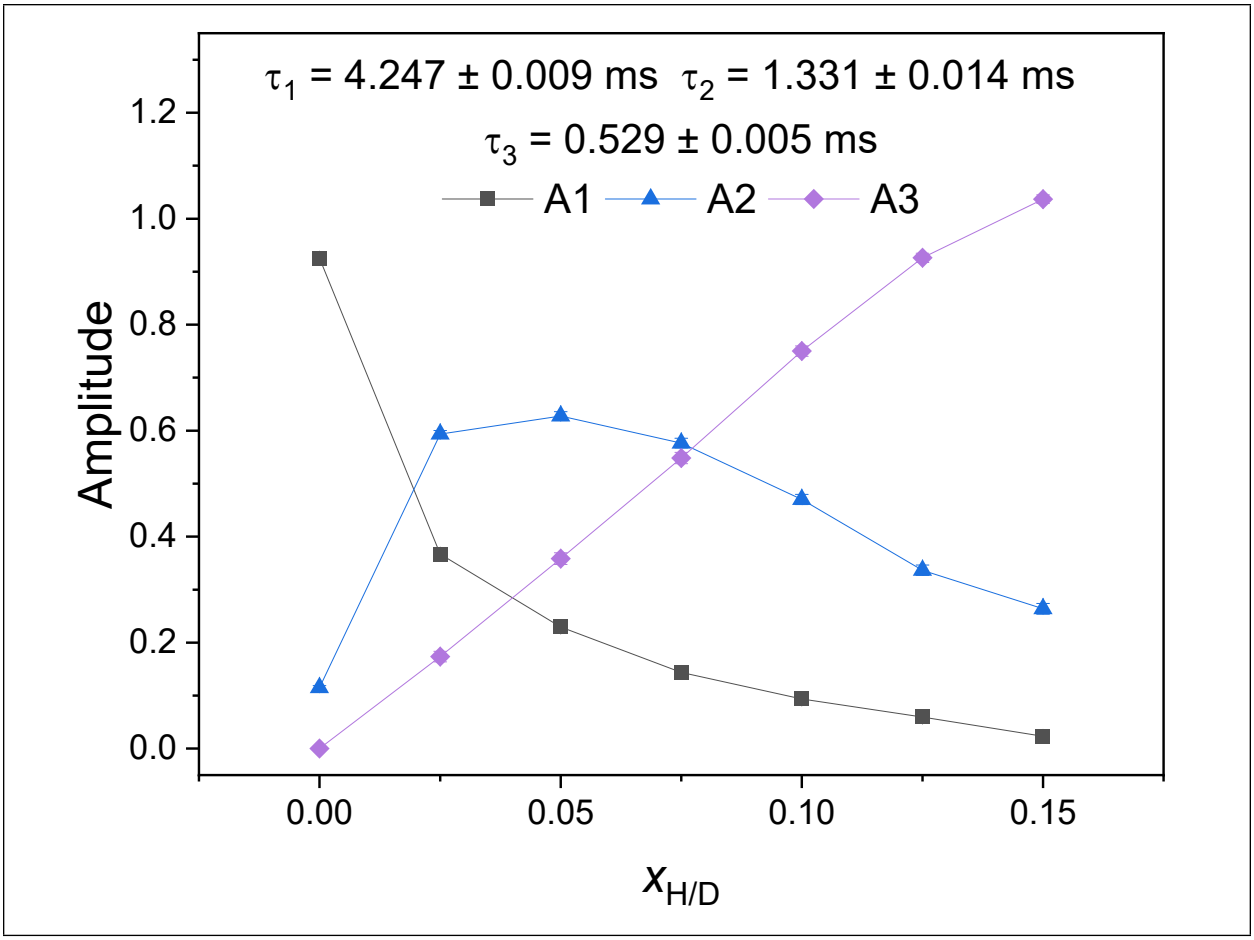

Figure S12. Amplitudes from global fit of $[Eu(H_2O)_9]^{3+}$ in mixtures of H_2O/D_2O in frozen solution at 77 K.

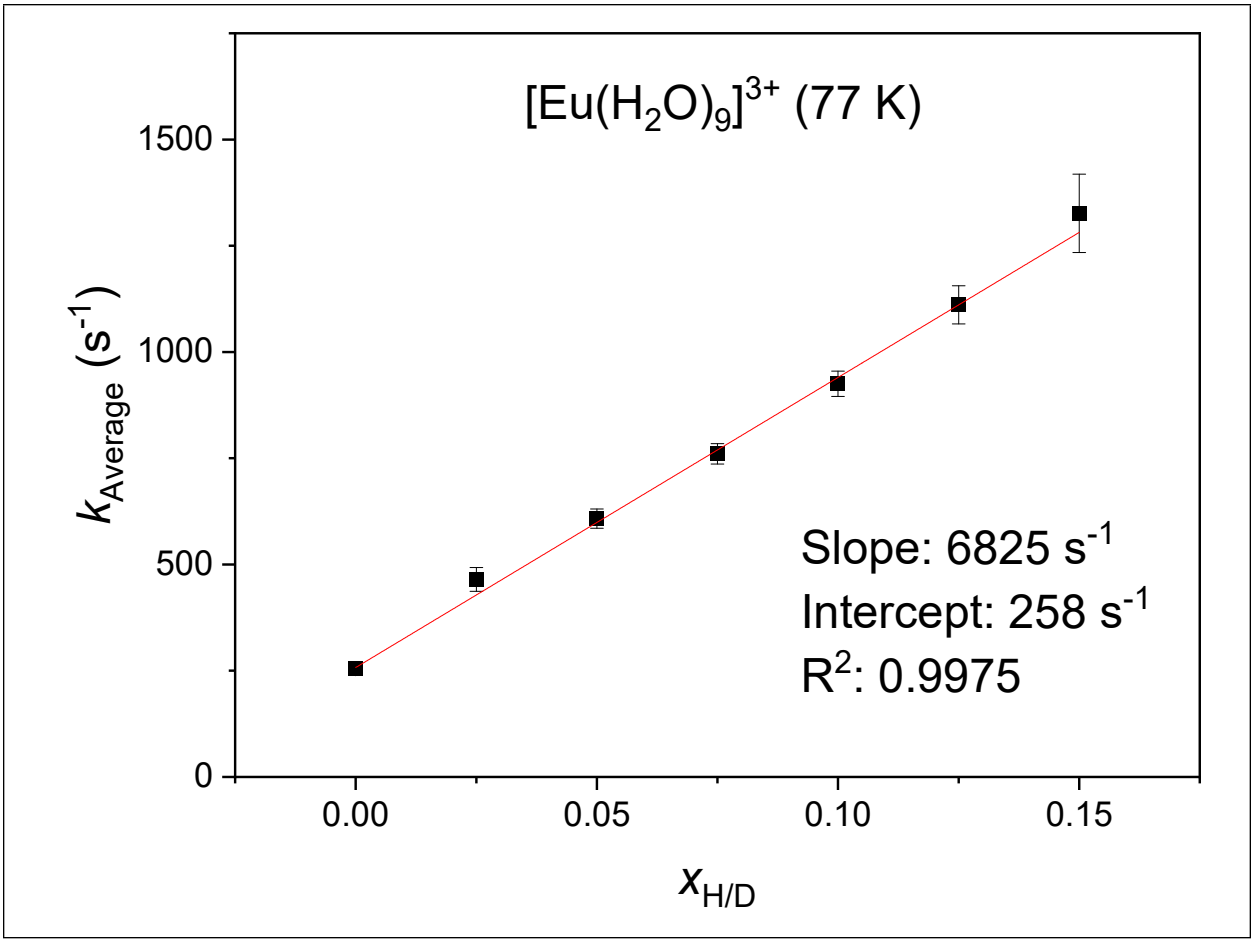

Figure S13. Average rate of deactivation ($k_{Average}$) of the $^5D_0$ state of $[Eu(H_2O)_9]^{3+}$ in H_2O/D_2O mixtures in frozen solution at 77 K obtained from a tri-exponential global fit. Data has been fitted with a linear function.

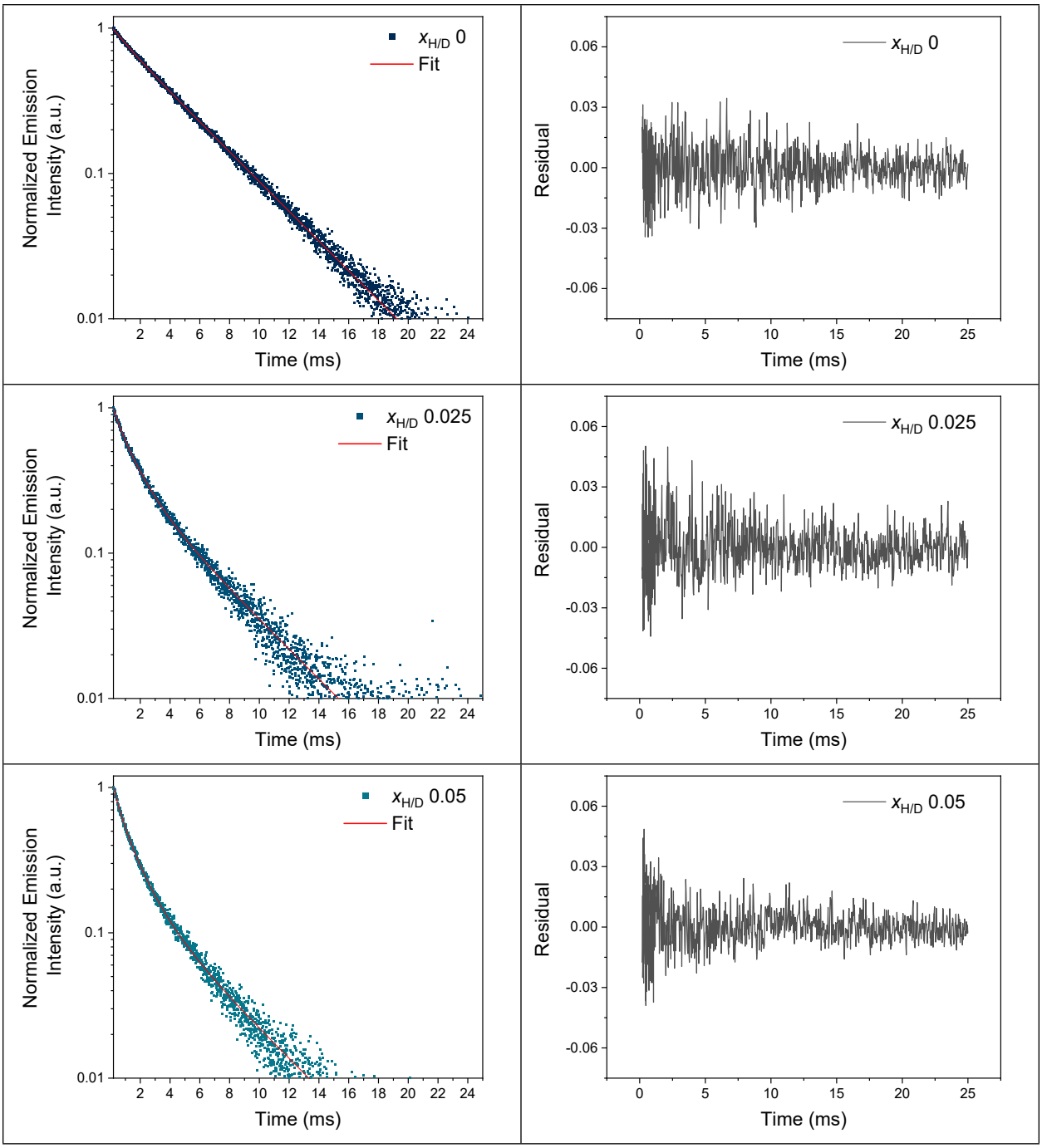
Normalized Emission Intensity (a.u.)
Time (ms)
$x_{H/D}$ 0
Fit
Residual
$x_{H/D}$ 0.025
$x_{H/D}$ 0.05

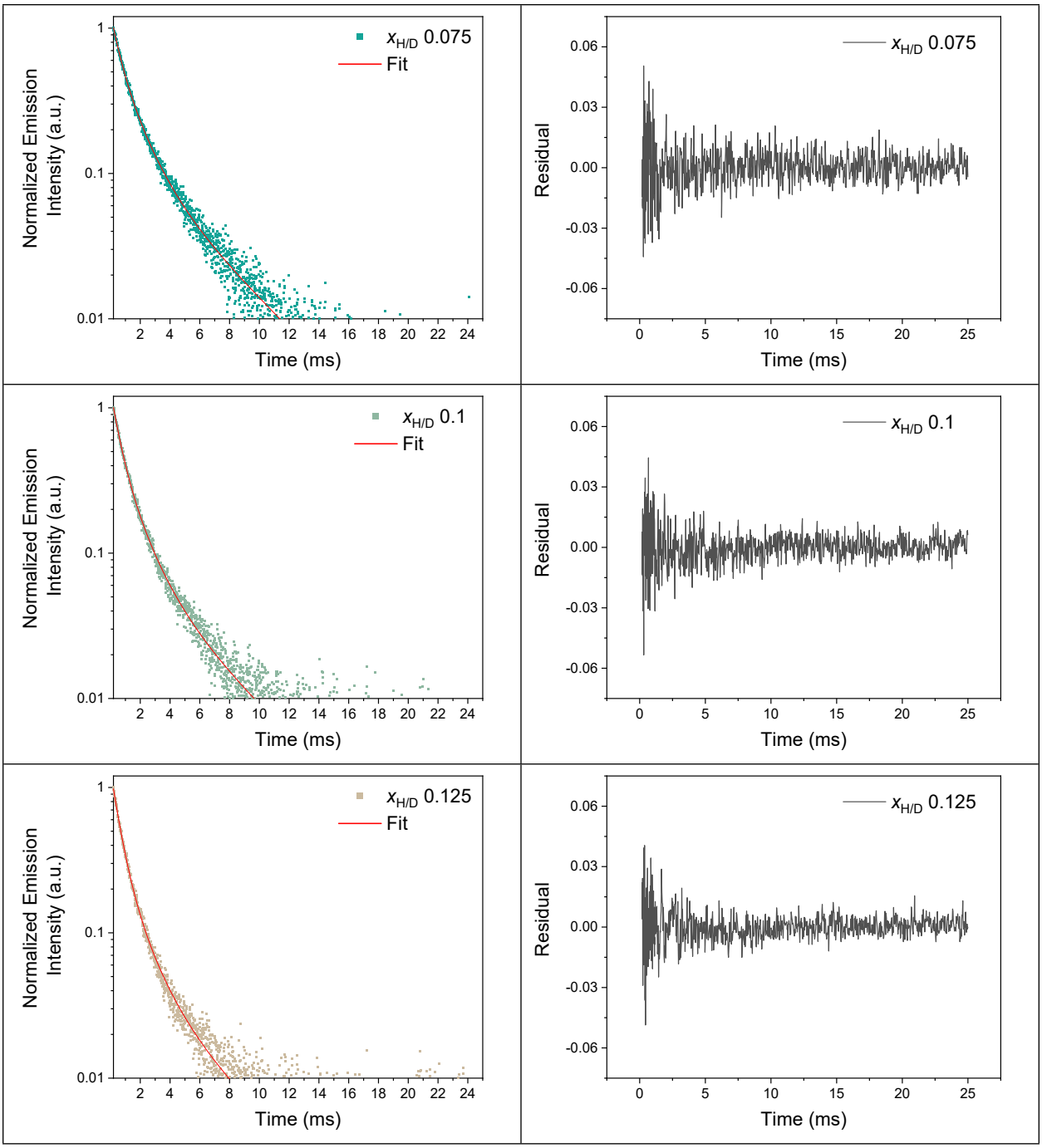
Normalized Emission Intensity (a.u.)
Time (ms)
$x_{H/D}$ 0.075
Fit
Residual
$x_{H/D}$ 0.1
$x_{H/D}$ 0.125

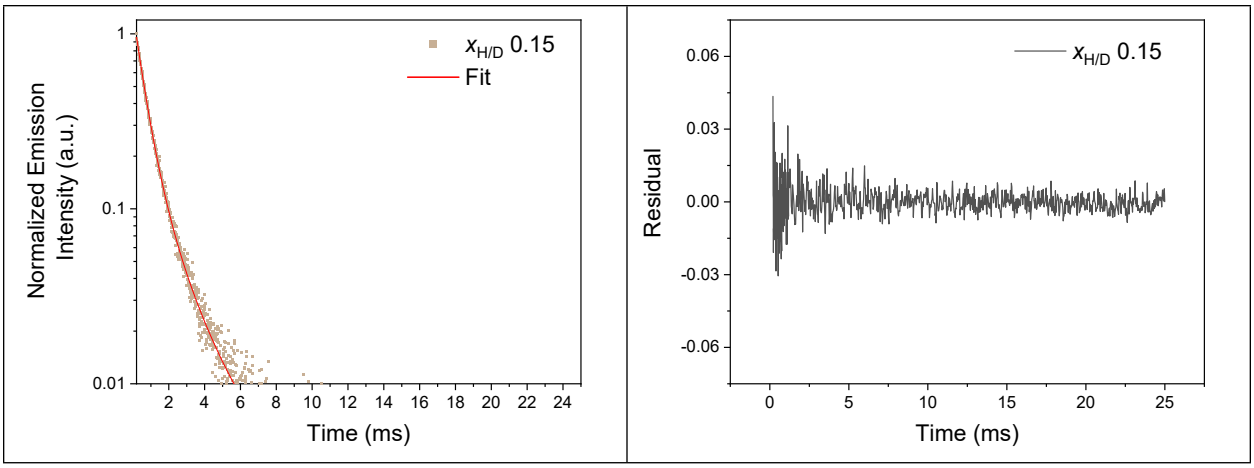

Figure S14. (left) Individual emission decay traces of $[Eu(H_2O)_9]^{3+}$ in H_2O/D_2O mixtures in frozen solution at 77 K. Data has been fitted to a tri-exponential decay with a global model (right) Residual of fit and data.

Table S4. Fit parameters for global fit of $[Eu(H_2O)_9]^{3+}$ at 77 K. *denotes fixed parameters

	τ_1	τ_2	τ_3
Global Parameter	4.247 ± 0.0090	1.331 ± 0.014	0.529 ± 0.0048
$x_{H/D}$	A_1	A_2	A_3
0	0.923 ± 0.0029	0.115 ± 0.0037	0 ± 0*
0.025	0.367 ± 0.0024	0.593 ± 0.007	0.174 ± 0.0099
0.05	0.229 ± 0.0021	0.627 ± 0.0083	0.358 ± 0.011
0.075	0.144 ± 0.0018	0.577 ± 0.0091	0.548 ± 0.011
0.1	0.0936 ± 0.0015	0.470 ± 0.0096	0.750 ± 0.0099
0.125	0.0594 ± 0.0013	0.337 ± 0.0098	0.926 ± 0.0088
0.15	0.0232 ± 0.0013	0.264 ± 0.010	1.04 ± 0.0083

[Eu(DOTA)(H_2O)]$^-$ / [Eu(DOTA)(D_2O)]$^-$

293 K

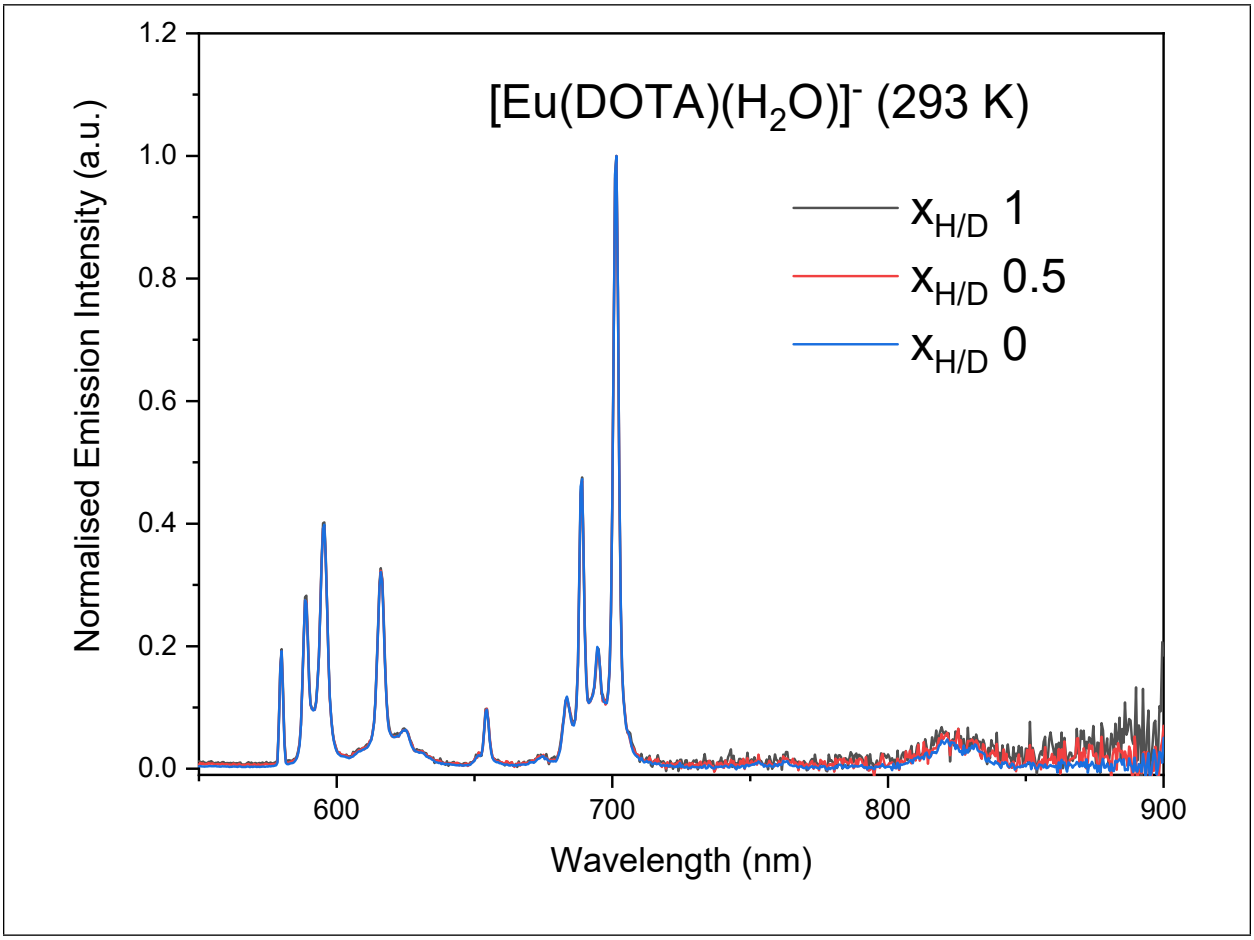

Figure S15. Normalised emission spectra of [Eu(DOTA)(H_2O)]$^-$ in mixtures of H_2O/D_2O in solution at 293 K. Emission slits were kept at 2 nm.

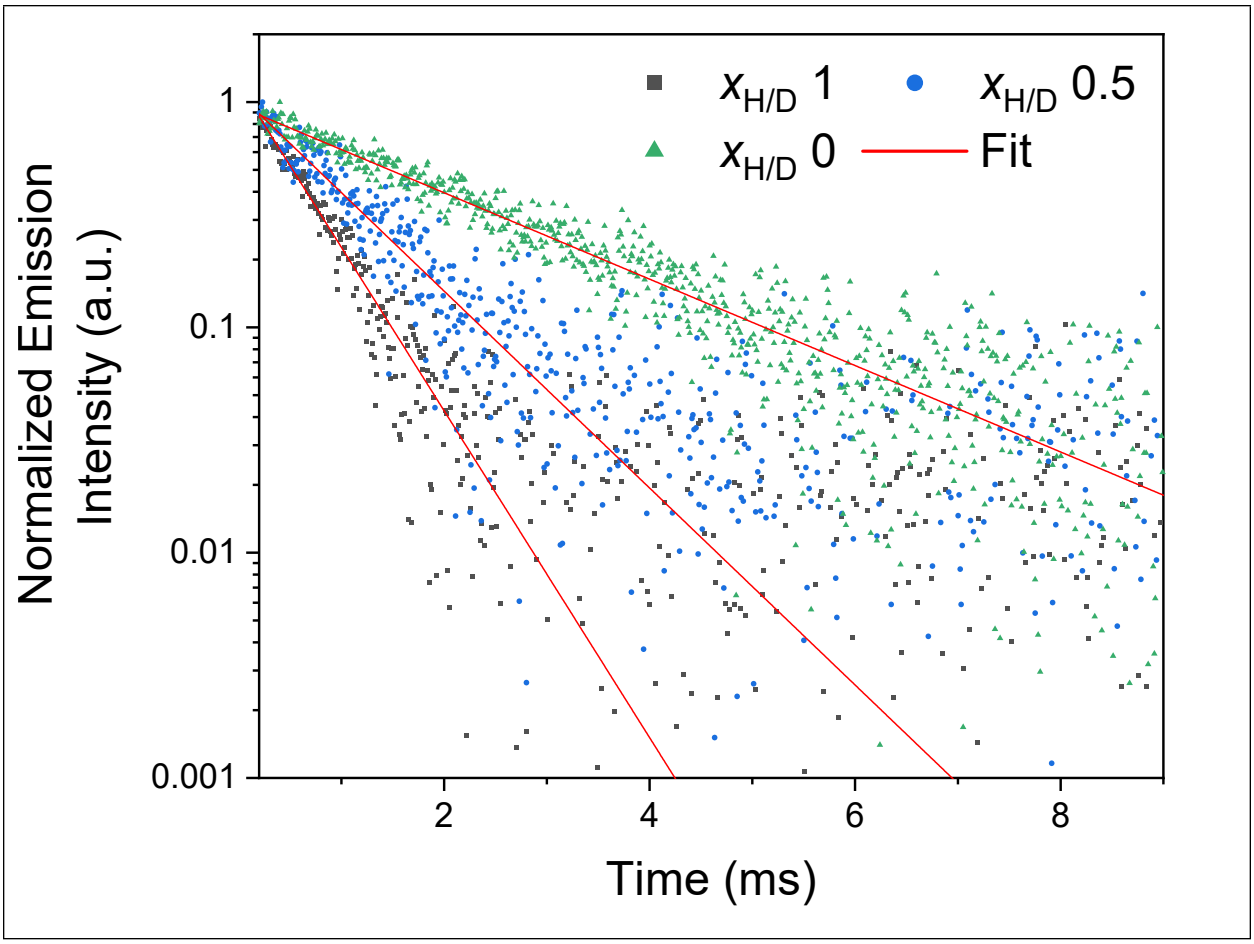

Figure S16. Emission decay traces of $[Eu(DOTA)(H_2O)]^-$ in mixtures of H_2O/D_2O in solution at 293 K. Data has been fitted with a mono-exponential decay function.

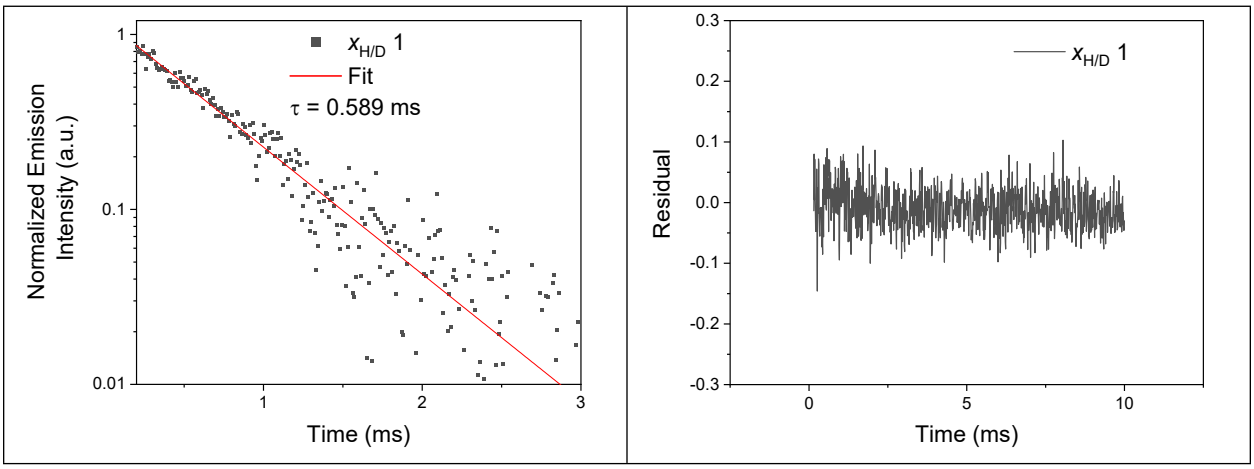

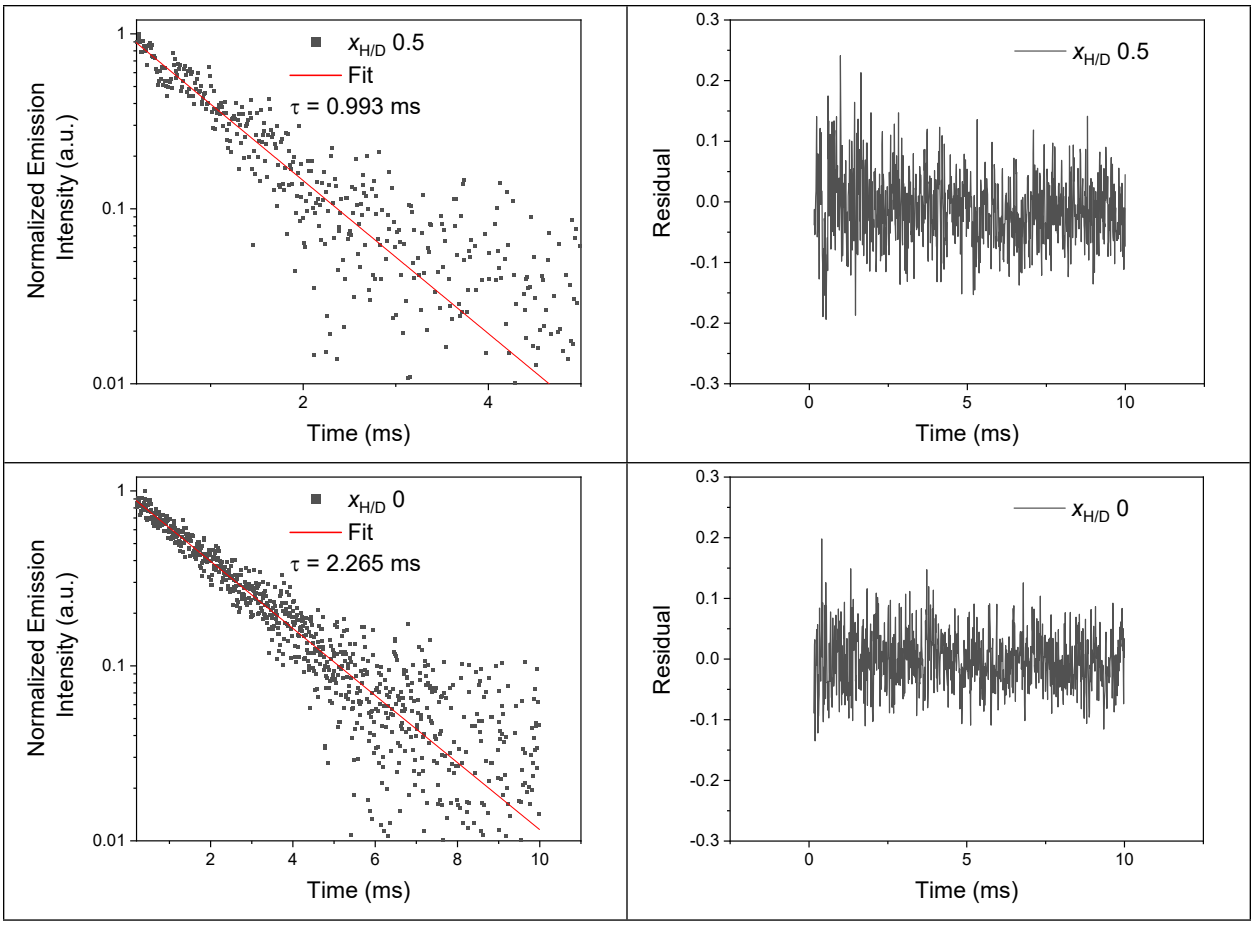

Figure S17. (left) Individual emission decay traces of $[Eu(DOTA)(H_2O)]^-$ in mixtures of H_2O/D_2O in solution at 293 K. Data has been fitted with a mono-exponential decay function. (right) Residual of fit and data.

Table S5. Fit parameters for of $[Eu(DOTA)(H_2O)]^-$ at 293 K

$x_{H/D}$	A	τ
1	1.21 ± 0.015	0.599 ± 0.0081
0.5	1.09 ± 0.016	0.993 ± 0.018
0	0.958 ± 0.0070	2.265 ± 0.022

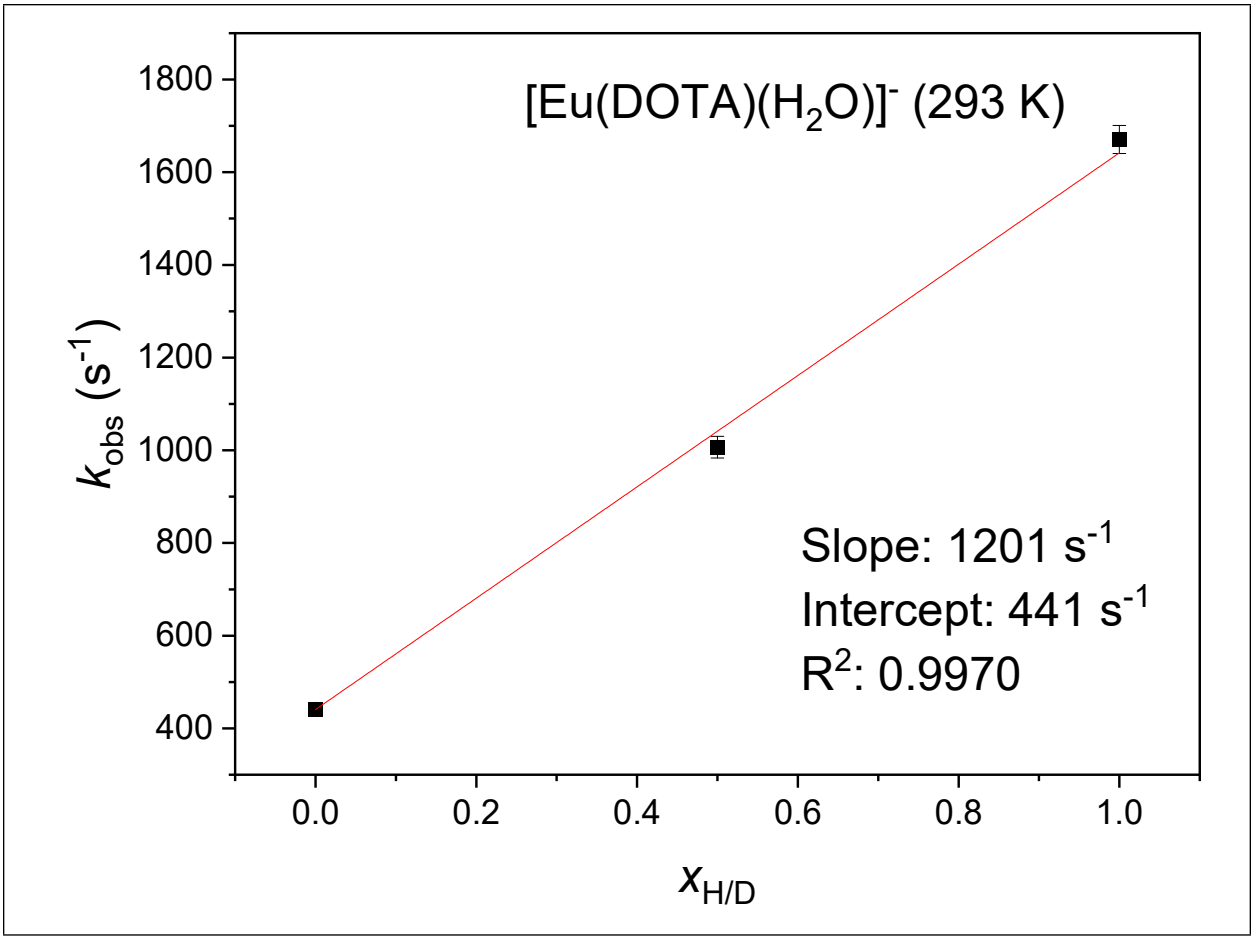

Figure S18. Observed rate of deactivation (k_{obs}) of the $^5D_0$ state of $[Eu(DOTA)(H_2O)]^-$ in mixtures of H_2O/D_2O in solution at 293 K. Data has been fitted with a linear function.

77 K

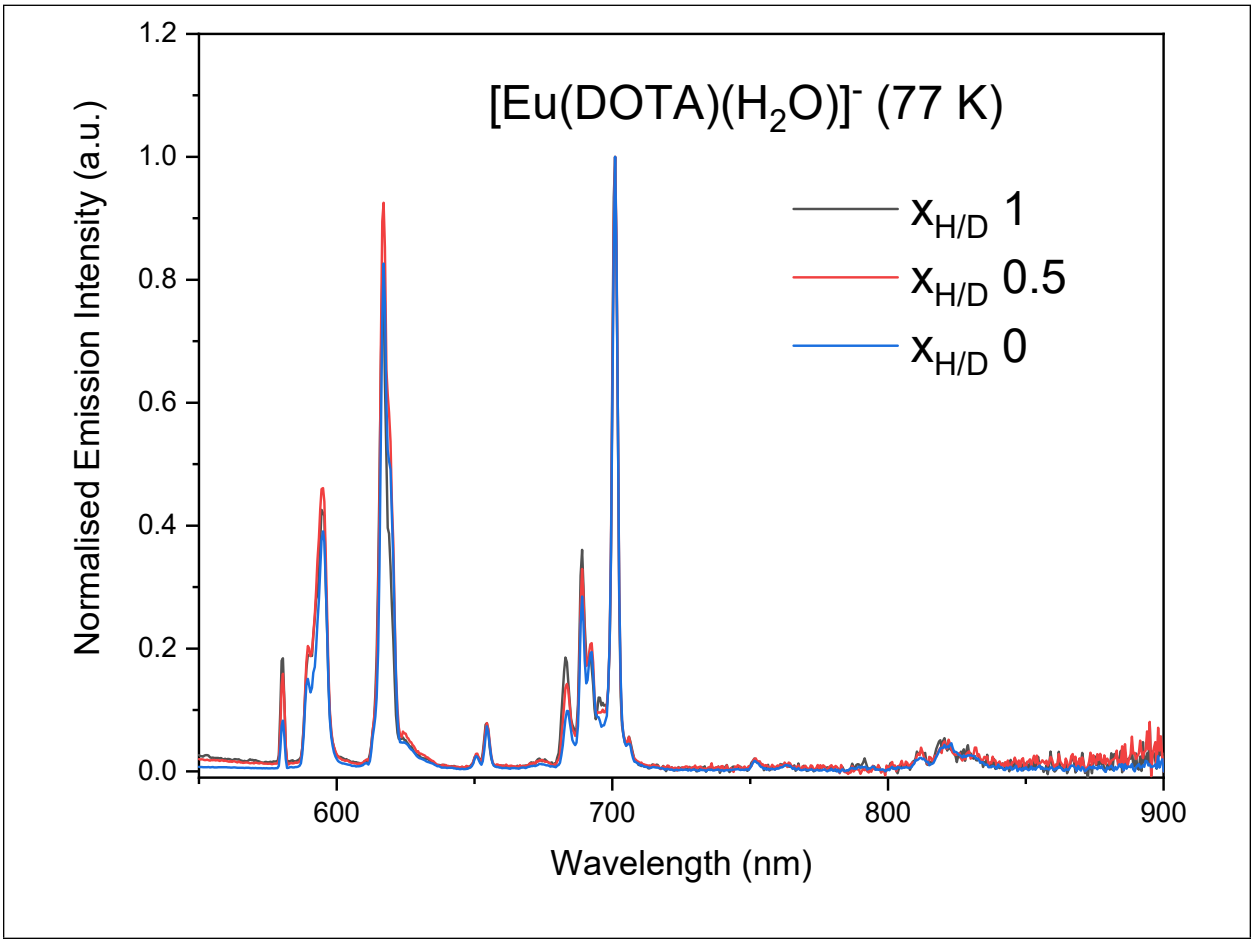

Figure S19. Normalised emission spectra of $[Eu(DOTA)(H_2O)]^-$ in mixtures of H_2O/D_2O in frozen solution at 77 K. Emission slits were kept at 2 nm.

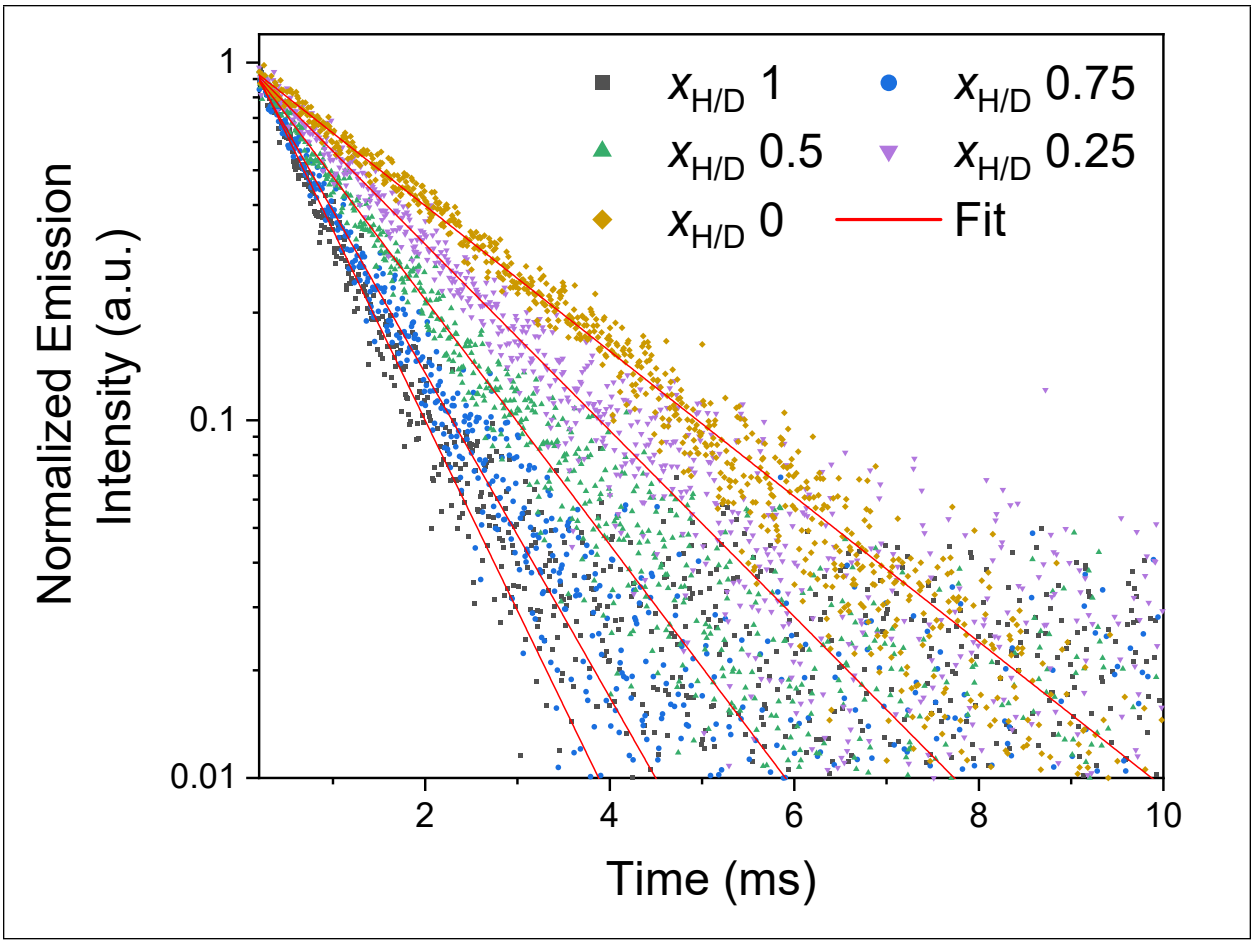

Figure S20. Emission decay traces of $[Eu(DOTA)(H_2O)]^-$ in mixtures of H_2O/D_2O in frozen solution at 77 K. Data has been fitted with a mono-exponential decay function.

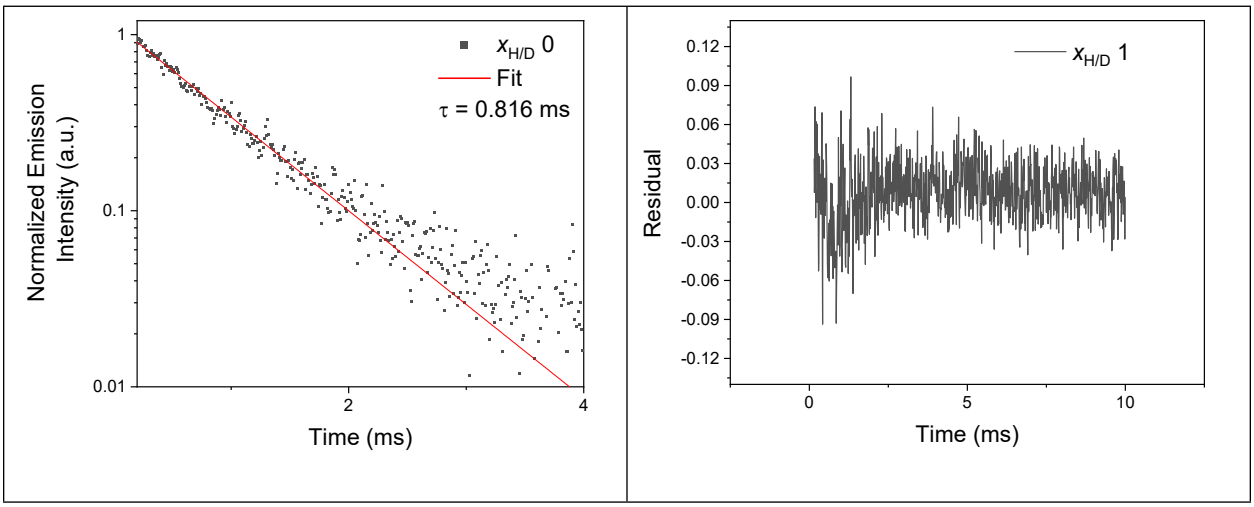

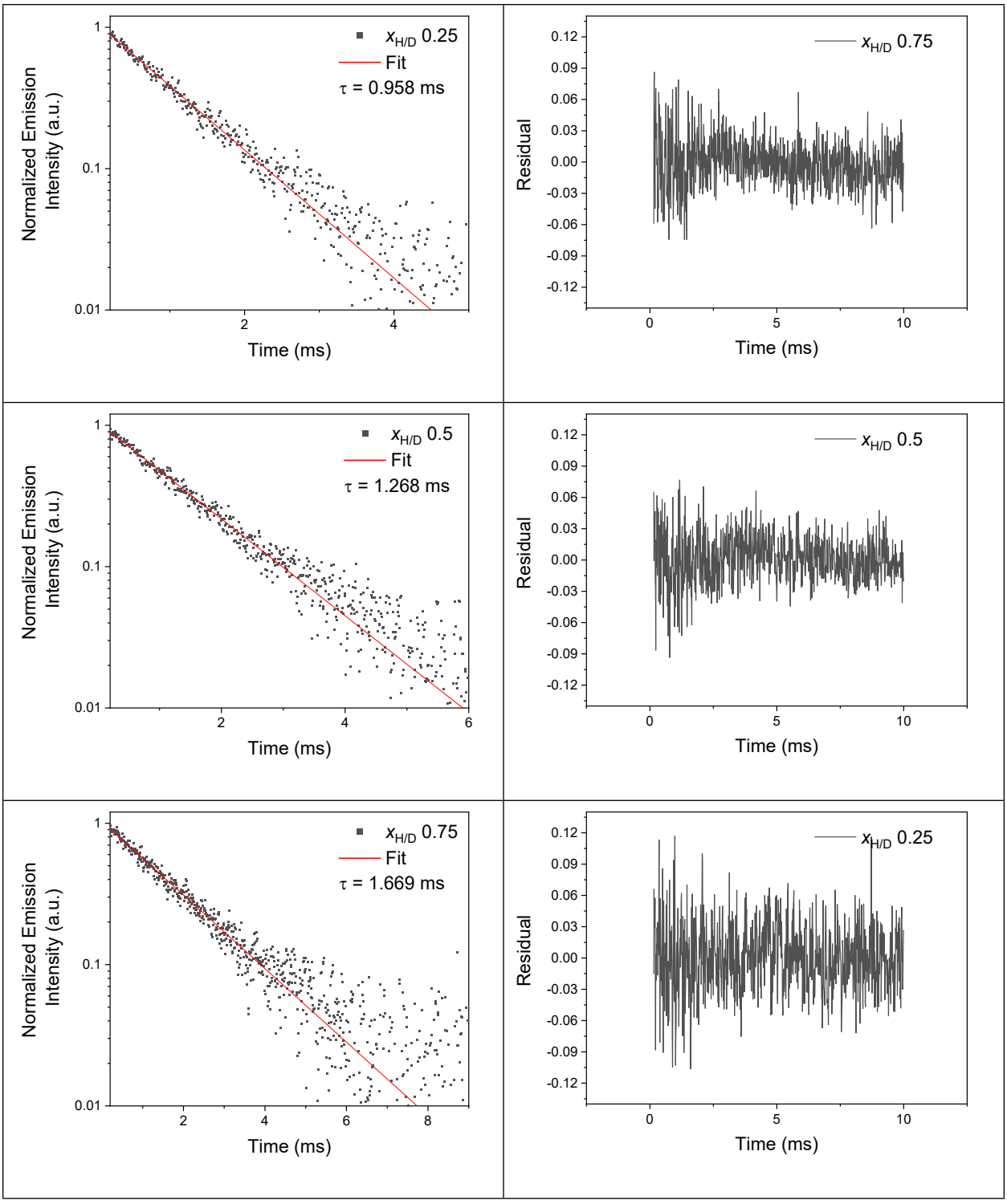
Normalized Emission Intensity (a.u.)
Time (ms)
$x_{H/D}$ 0.25
Fit
τ = 0.958 ms
Residual
$x_{H/D}$ 0.75
$x_{H/D}$ 0.5
Fit
τ = 1.268 ms
$x_{H/D}$ 0.5
$x_{H/D}$ 0.75
Fit
τ = 1.669 ms
$x_{H/D}$ 0.25

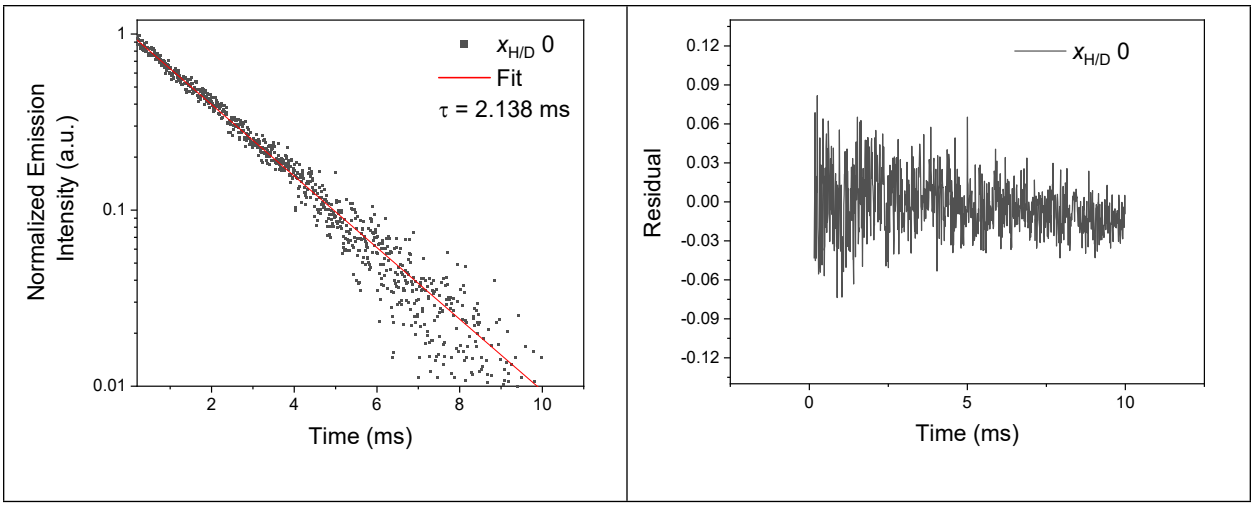

Figure S21. (left) Individual emission decay traces of $[Eu(DOTA)(H_2O)]^-$ in mixtures of H_2O/D_2O in frozen solution at 77 K. Data has been fitted with a mono-exponential decay function. (right) Residual of fit and data.

Table S6. Fit parameters for of $[Eu(DOTA)(H_2O)]^-$ at 77 K

$x_{H/D}$	A	τ
1	1.16 ± 0.0075	0.816 ± 0.0062
0.75	1.09 ± 0.0062	0.958 ± 0.0066
0.5	1.05 ± 0.0049	1.268 ± 0.0074
0.25	1.03 ± 0.0057	1.669 ± 0.012
0	1.01 ± 0.0035	2.138 ± 0.0097

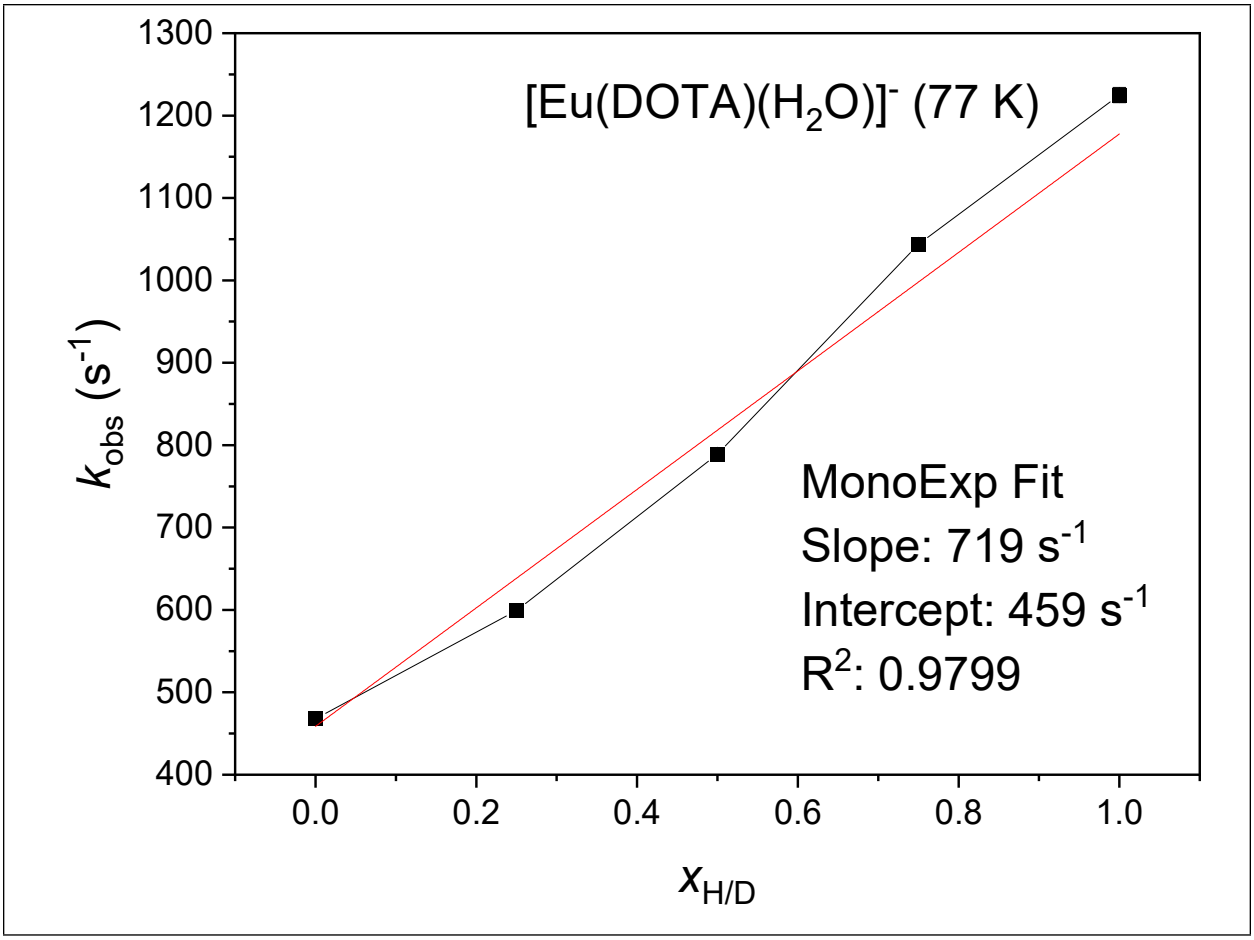

Figure S22. Observed rate of deactivation (k_{obs}) of the $^5D_0$ state of $[Eu(DOTA)(H_2O)]^-$ in mixtures of H_2O/D_2O in frozen solution at 77 K. Obtained from mono-exponential fit. Data has been fitted with a linear function.

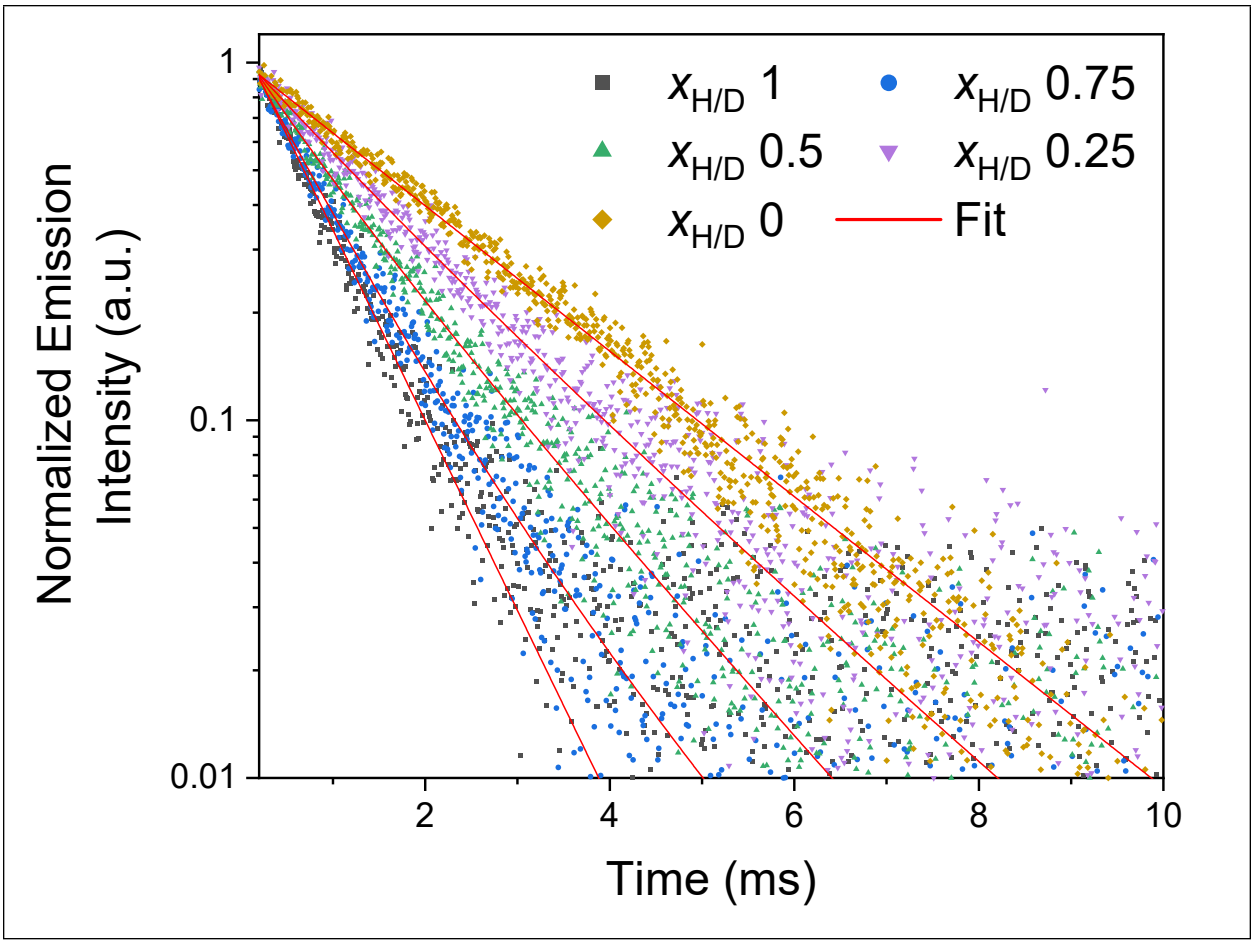

Figure S23. Emission decay traces of $[Eu(DOTA)(H_2O)]^-$ in mixtures of H_2O/D_2O in frozen solution at 77 K. Data has been fitted globally with a tri-exponential decay function.

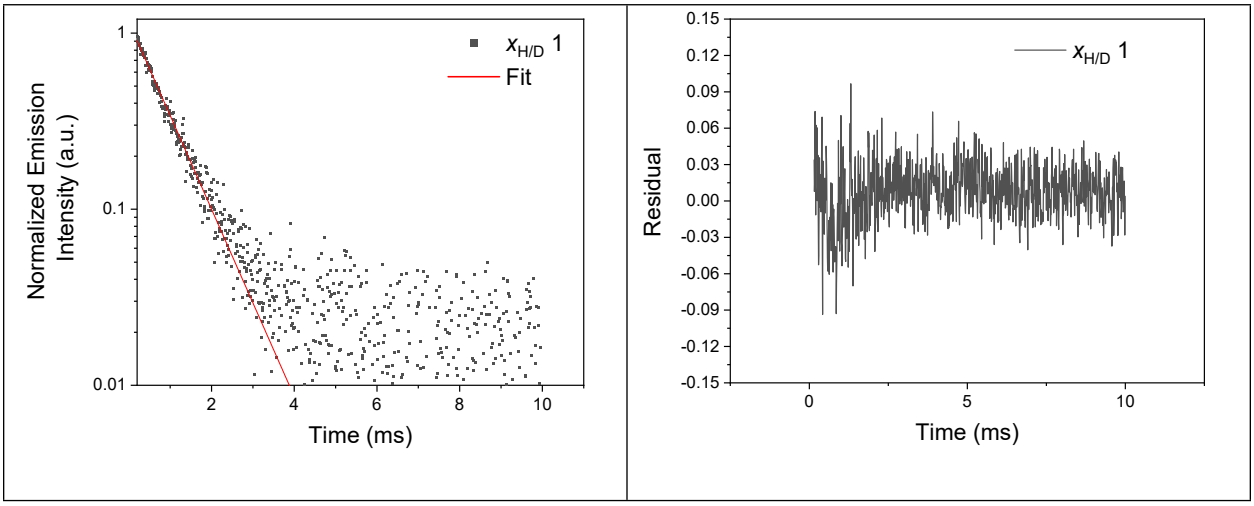

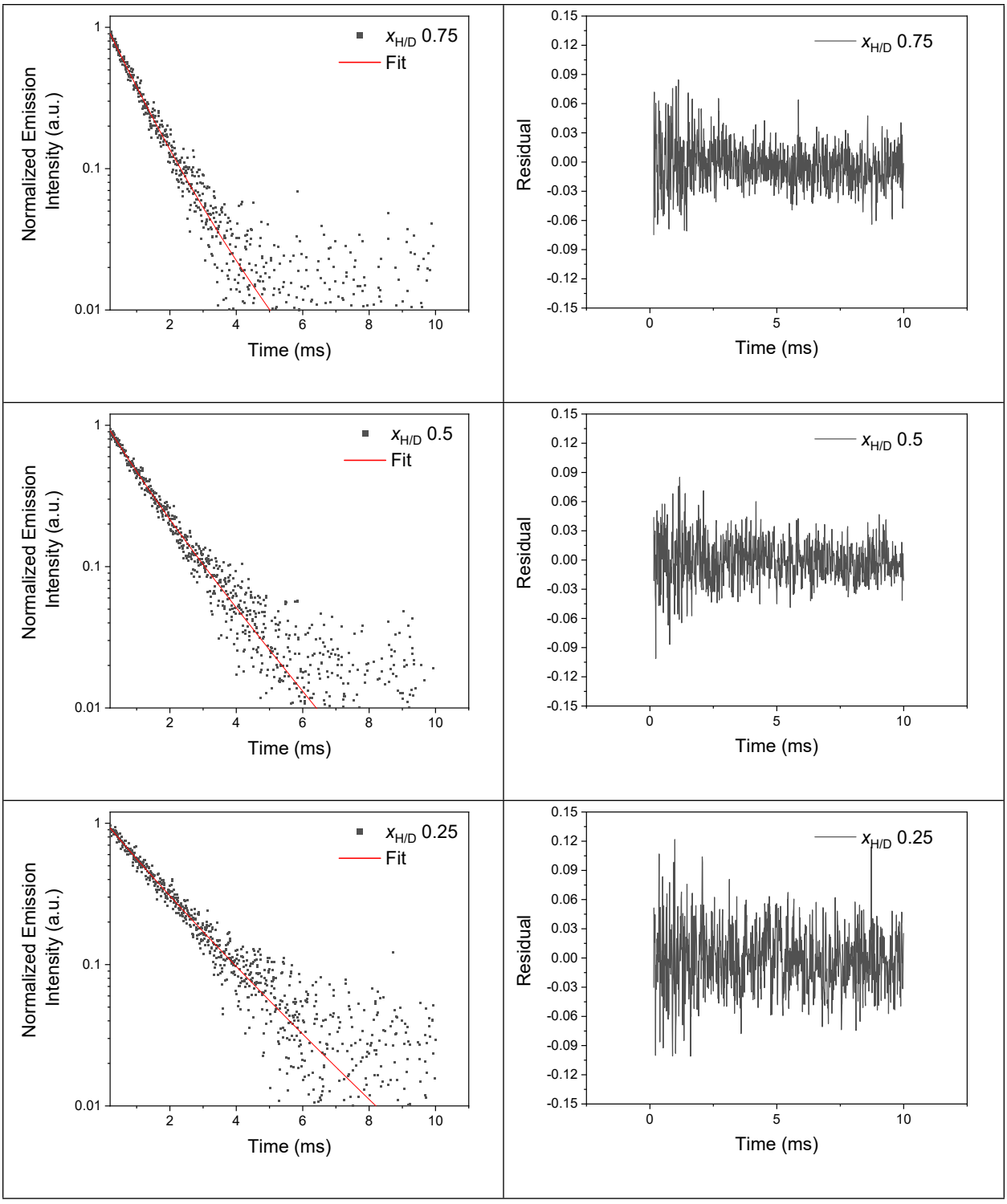
Normalized Emission Intensity (a.u.)
Time (ms)
$x_{H/D}$ 0.75
Fit
Residual
$x_{H/D}$ 0.5
$x_{H/D}$ 0.25

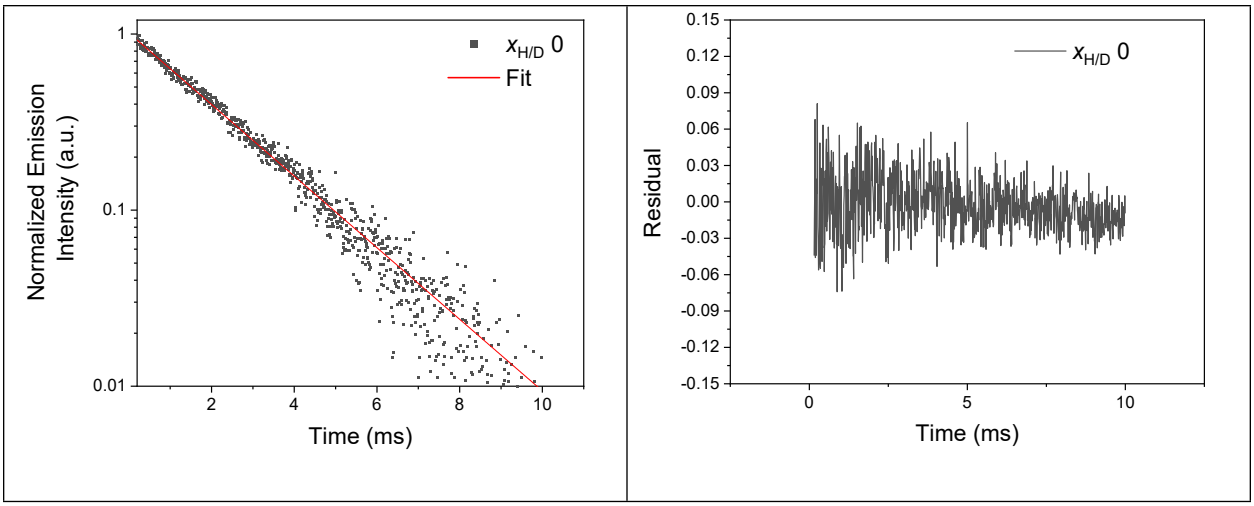

Figure S24. (left) Individual emission decay traces of $[Eu(DOTA)(H_2O)]^-$ in mixtures of H_2O/D_2O in frozen solution at 77 K. Data has been fitted globally with a tri-exponential decay function. (right) Residual of fit and data.

Table S7. Fit parameters for global fit of $[Eu(DOTA)(H_2O)]^-$ at 77 K. * denotes fixed parameters.

	τ_1	τ_2	τ_3
Global Parameter	0.817 ± 0.006	1.518 ± 0.206	2.136 ± 0.065
$x_{H/D}$	A_1	A_2	A_3
1	1.16 ± 0.0076	0 ± 0*	0 ± 0*
0.75	0.906 ± 0.045	0.218 ± 0.067	0 ± 0.058
0.5	0.443 ± 0.087	0.669 ± 0.093	0 ± 0.15
0.25	0.0946 ± 0.082	0.624 ± 0.11	0.334 ± 0.15
0	0 ± 0*	0 ± 0.11	1.01 ± 0.11

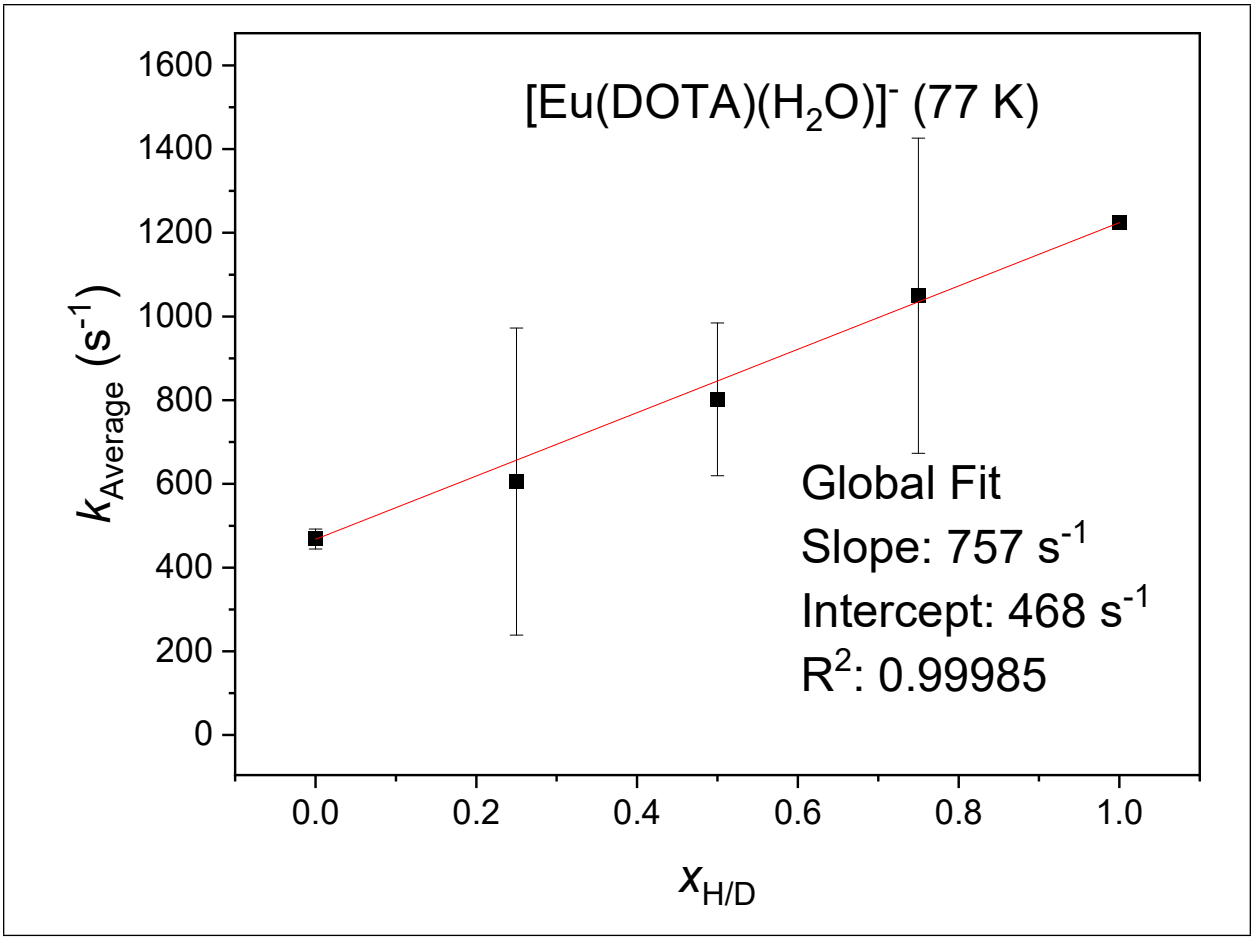

Figure S25. Average rate of deactivation ($k_{Average}$) of the $^5D_0$ state of $[Eu(DOTA)(H_2O)]^-$ in mixtures of H_2O/D_2O in frozen solution at 77 K obtained from amplitude averaged excited state lifetimes of global fit. Data has been fitted with a linear function.

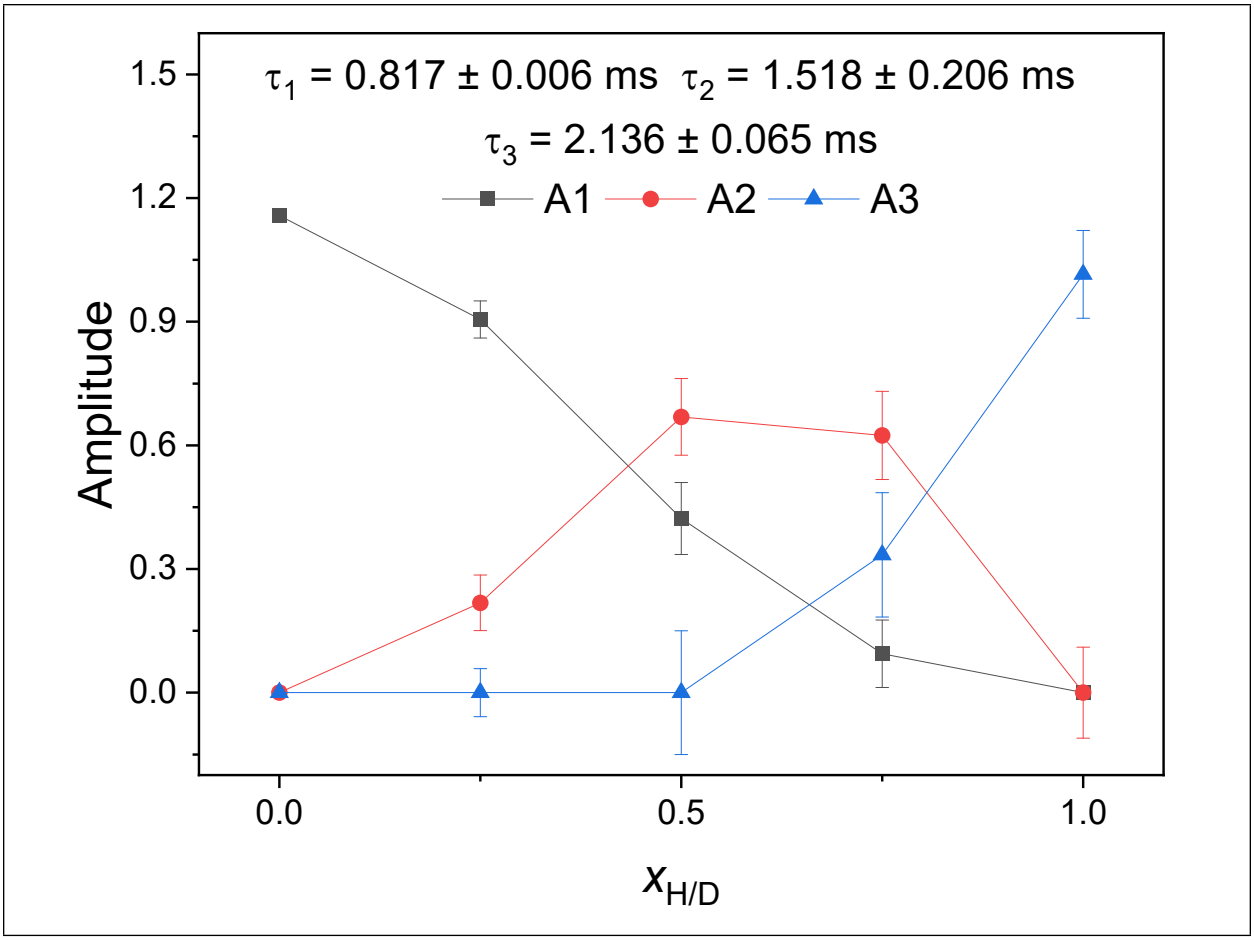

Figure S26. Amplitudes from global fit of $[Eu(DOTA)(H_2O)]^-$ in mixtures of H_2O/D_2O in frozen solution at 77 K.

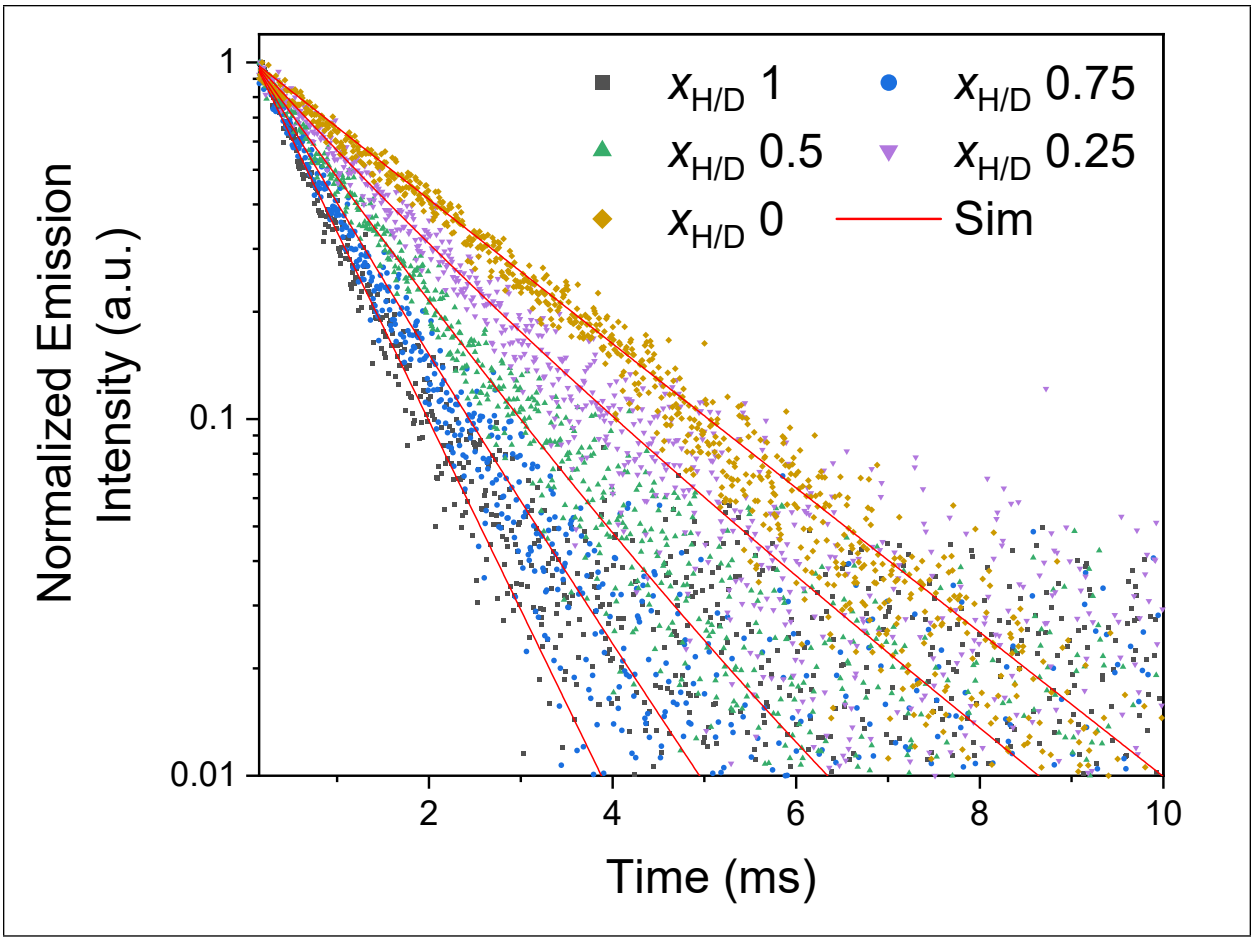

Figure S27. Emission decay traces of $[Eu(DOTA)(H_2O)]^-$ in mixtures of H_2O/D_2O in frozen solution at 77 K with simulated data using a 3-component model.

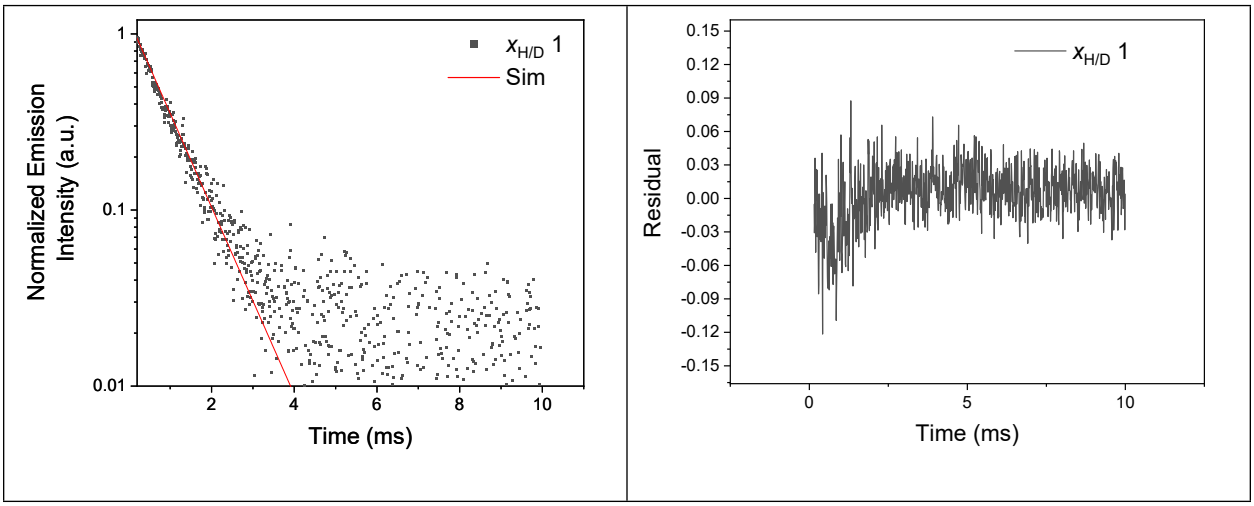

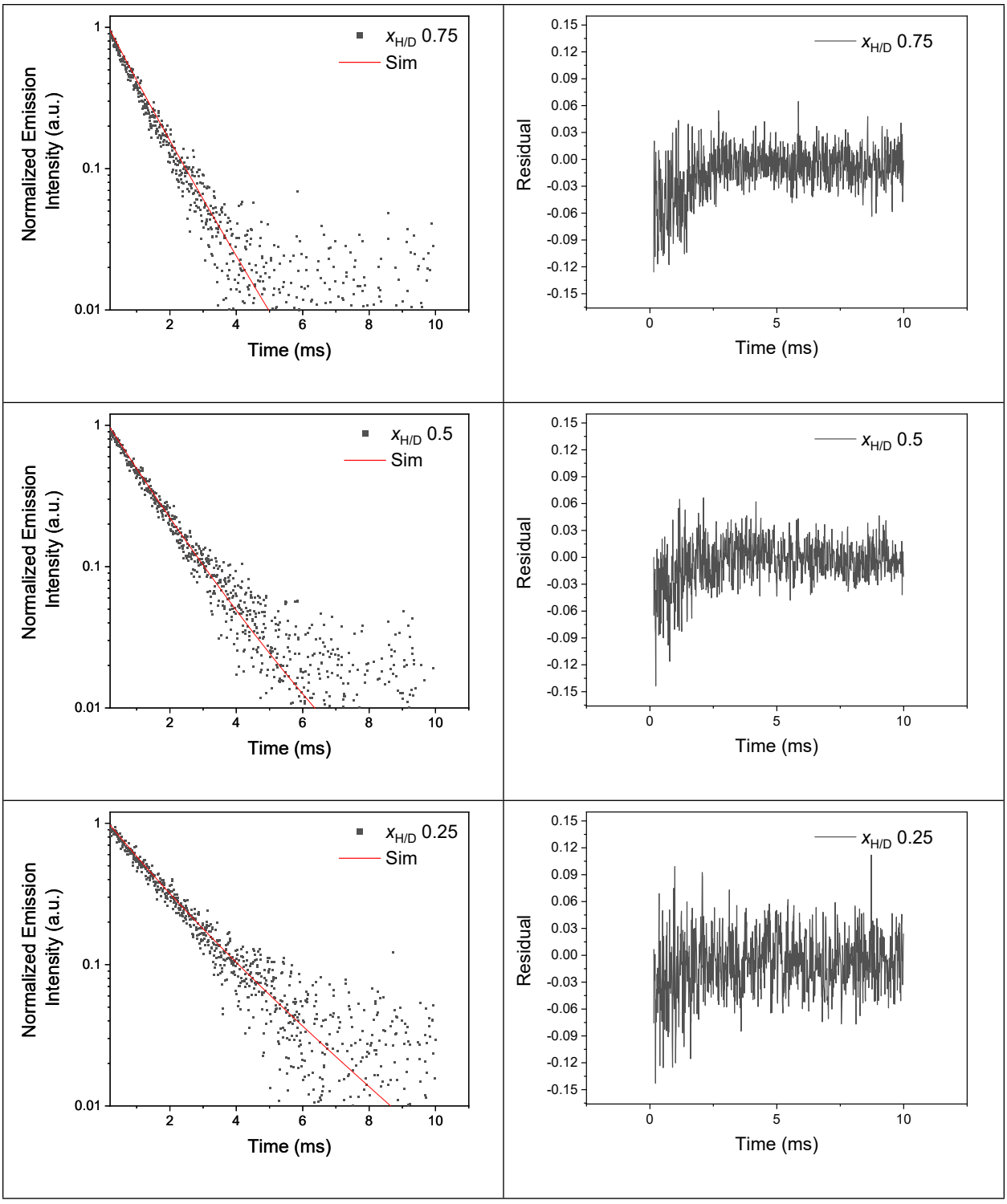
Normalized Emission Intensity (a.u.)
Time (ms)
$x_{H/D}$ 0.75
Sim
Residual
$x_{H/D}$ 0.5
$x_{H/D}$ 0.25

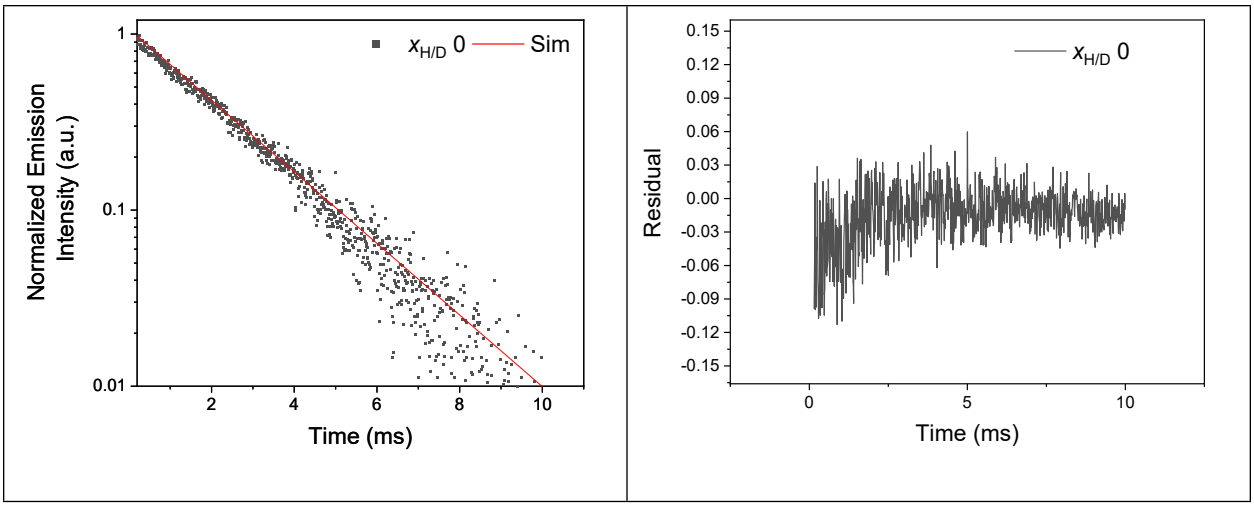

Figure S28. (left) Individual emission decay traces of $[Eu(DOTA)(H_2O)]^-$ in mixtures of H_2O/D_2O in frozen solution at 77 K with simulated data using a 3-component model. (right) Residual between simulation and data.

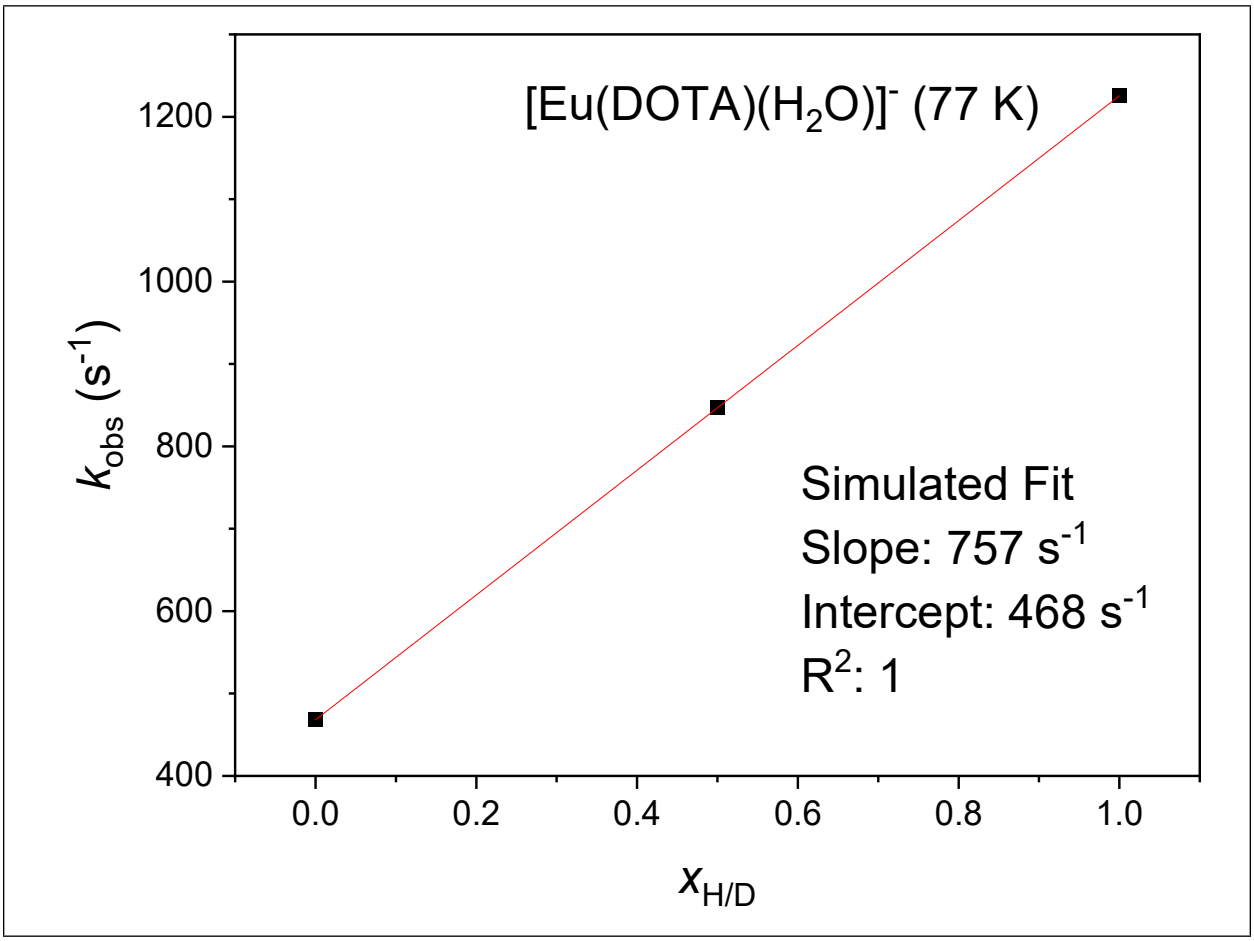

Figure S29. Observed rate of deactivation (k_{obs}) of the $^5D_0$ state of $[Eu(DOTA)(H_2O)]^-$ obtained from excited state lifetimes used in the simulated fits.

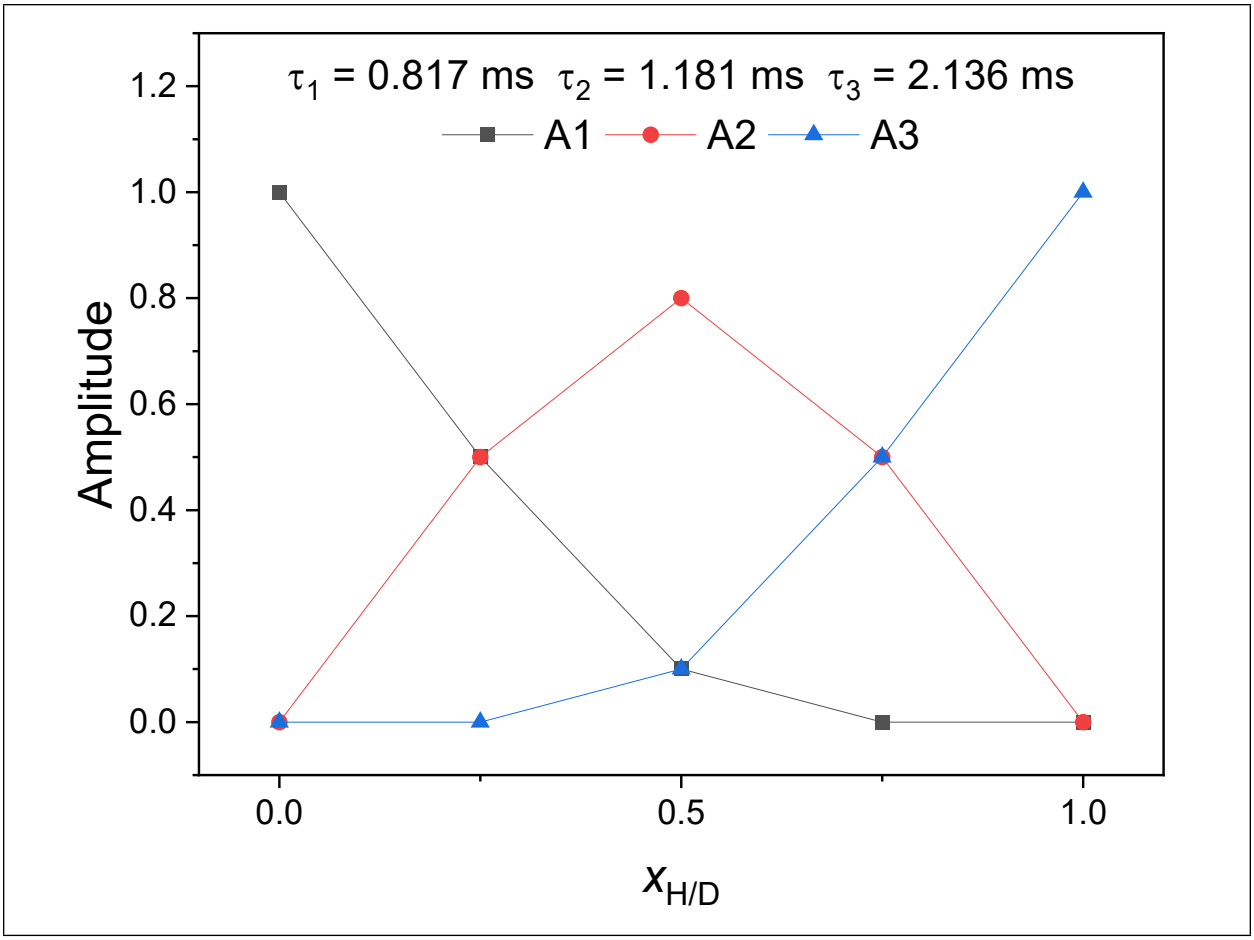

Figure S30. Amplitudes used in simulated excited state lifetimes of $[Eu(DOTA)(H_2O)]^-$.

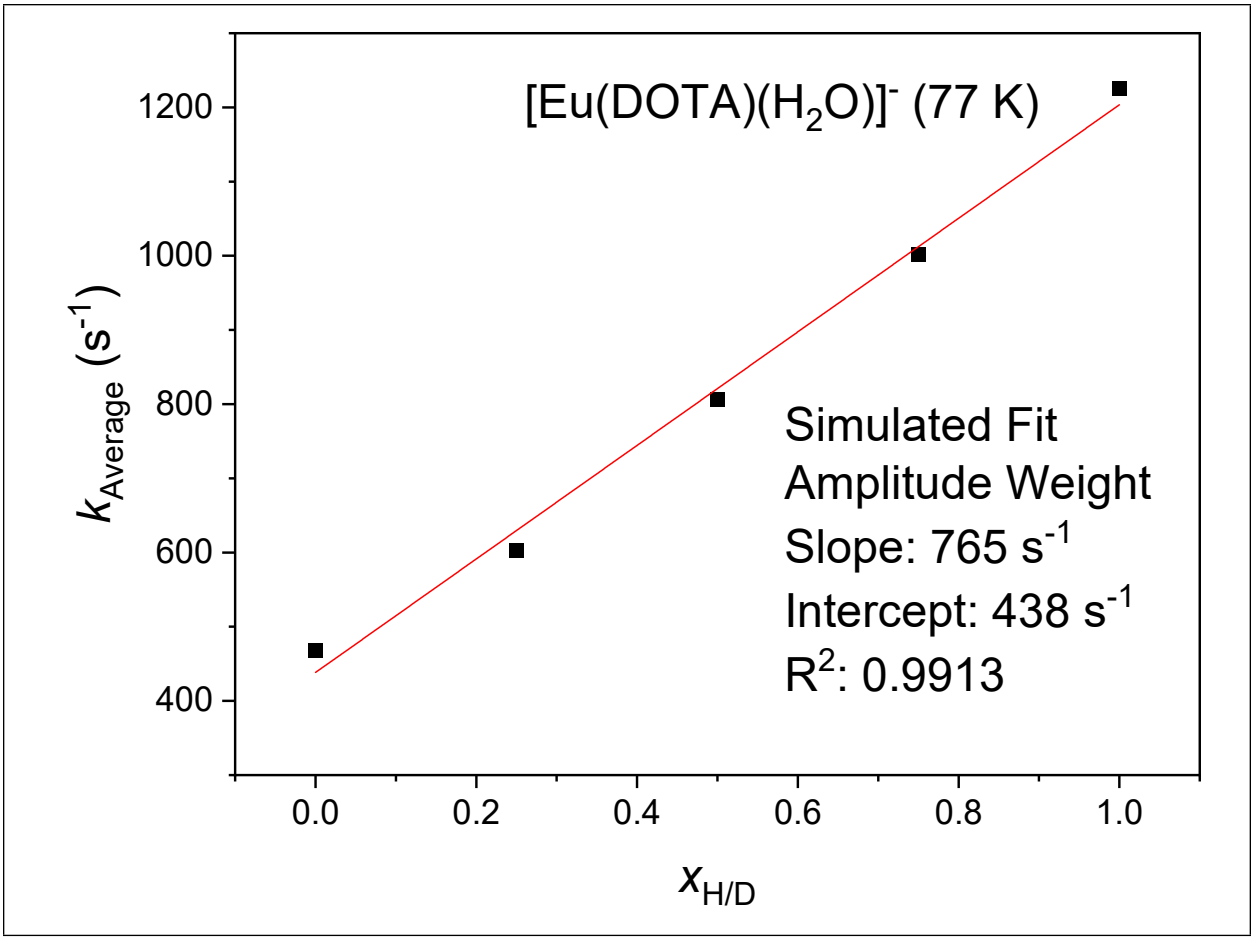

Figure S31. Average rate of deactivation ($k_{Average}$) of the $^5D_0$ state of $[Eu(DOTA)(H_2O)]^-$. Obtained from amplitude-weighted averages of simulated lifetimes. Data has been fitted with a linear function

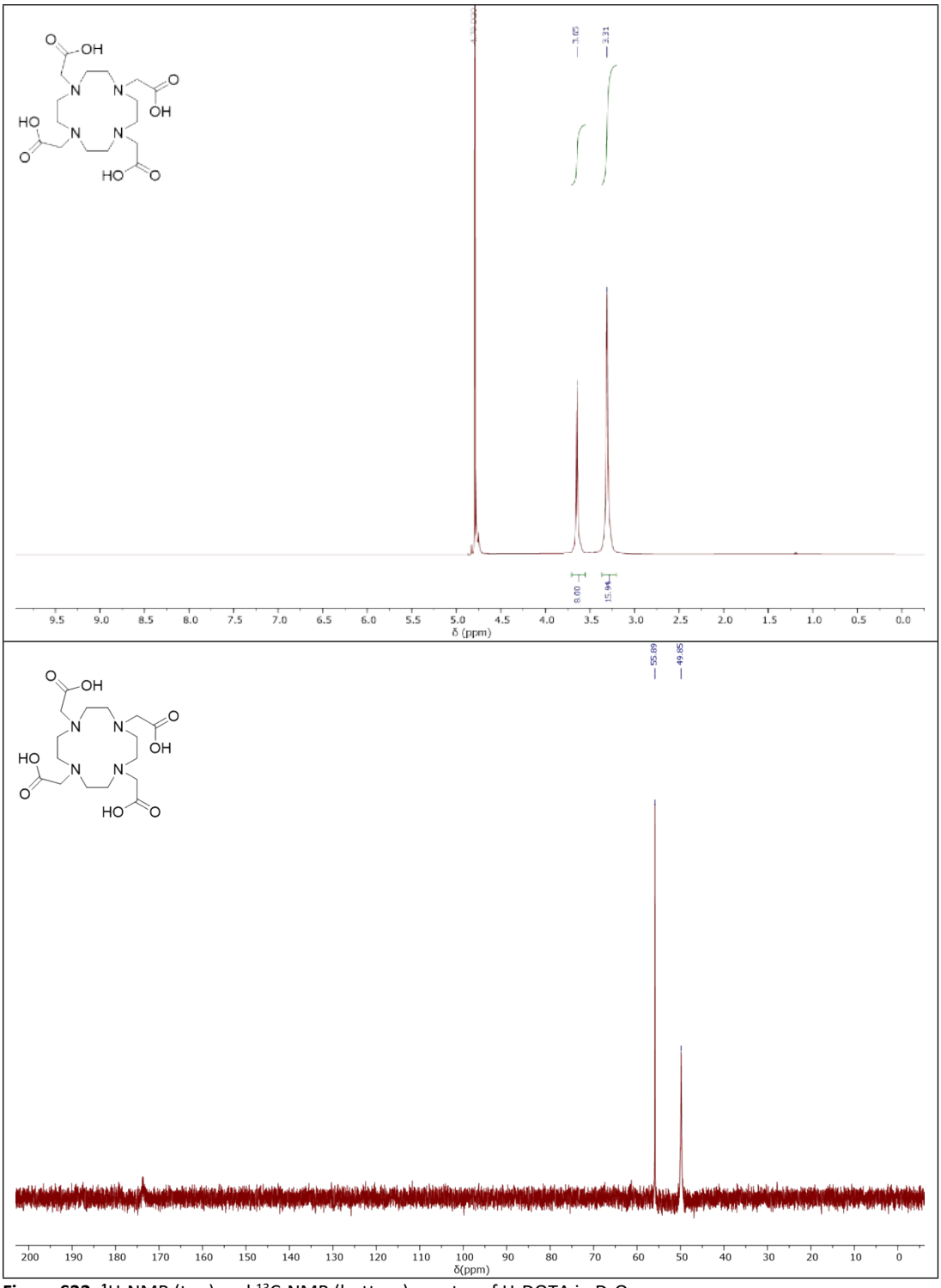

Figure S32. ^{1}H-NMR (top) and ^{13}C-NMR (bottom) spectra of H_4DOTA in D_2O.

^{1}H-NMR (500 MHz, D_2O) δ 3.65 (s, 8H), 3.31 (s, 16H).
^{13}C-NMR (126 MHz, D_2O) δ 55.89, 49.85.
HRMS (ESI^+): m/z calculated for $C_{16}H_{28}N_4O_8$ $[M+H]^+$: 405.1907; found 405.1990.

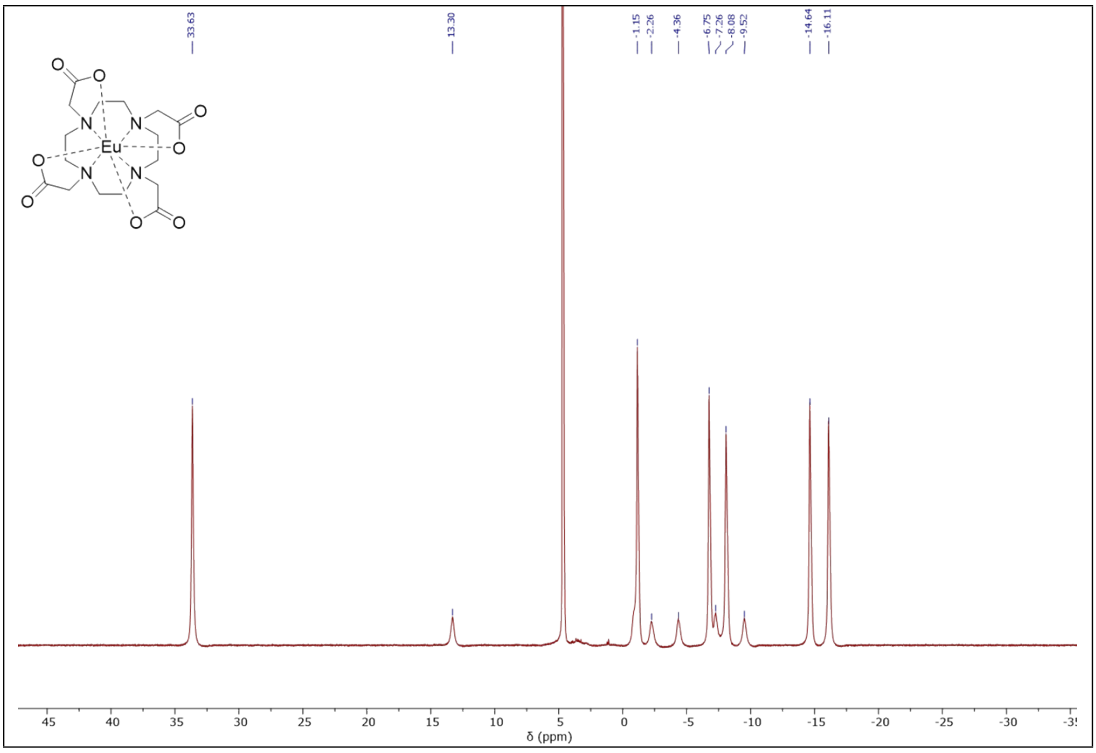

Figure S33. Paramagnetic 1H-NMR spectra of $[Eu(DOTA)(D_2O)]^-$ in D_2O.

^{1}H NMR (500 MHz, D_2O) δ 33.63, -1.15, -6.75, -8.09, -14.63, -16.11 (SAP). 13.30, -2.26, -4.36, -7.26, -9.52 (TSAP). **HRMS** (ESP^+): m/z calculated for $C_{16}H_{24}N_4O_8Eu$ $[M+2H]^+$: 555.0959, found: 555.0977.

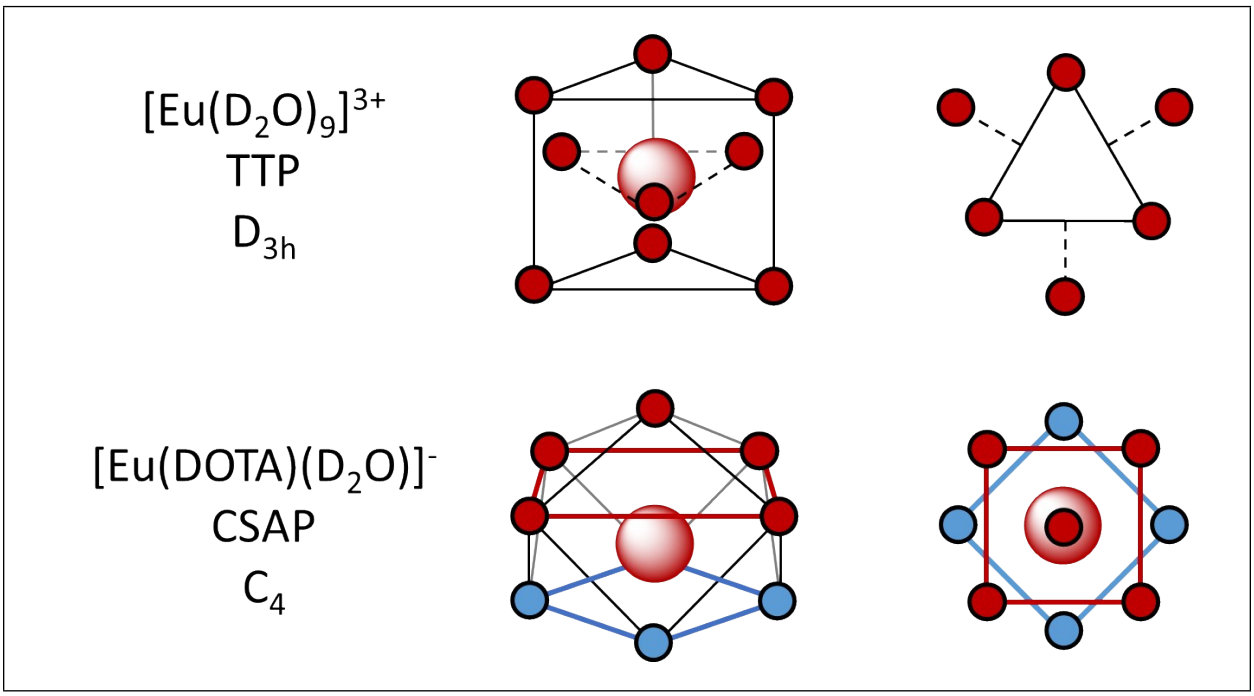

Figure S34. Schematic of the structure and symmetry of $[Eu(D_2O)_9]^{3+}$ (top) and $[Eu(DOTA(D_2O)]^-$ (bottom).